Mechanisms for the Extraction of Tropopause Polar Vortices and Associated Surface-based Pools of Arctic Air from High Latitudes and their Transport to Middle Latitudes

Kevin A. Biernat

Department of Atmospheric and Environmental Sciences

University at Albany, SUNY

ATM 619 Project Presentation

3 May 2016

What are Tropopause Polar Vortices (TPVs)?

- TPVs are defined as tropopause-based vortices of high-latitude origin and are material features (Pyle et al. 2004; Cavallo and Hakim 2009, 2010)

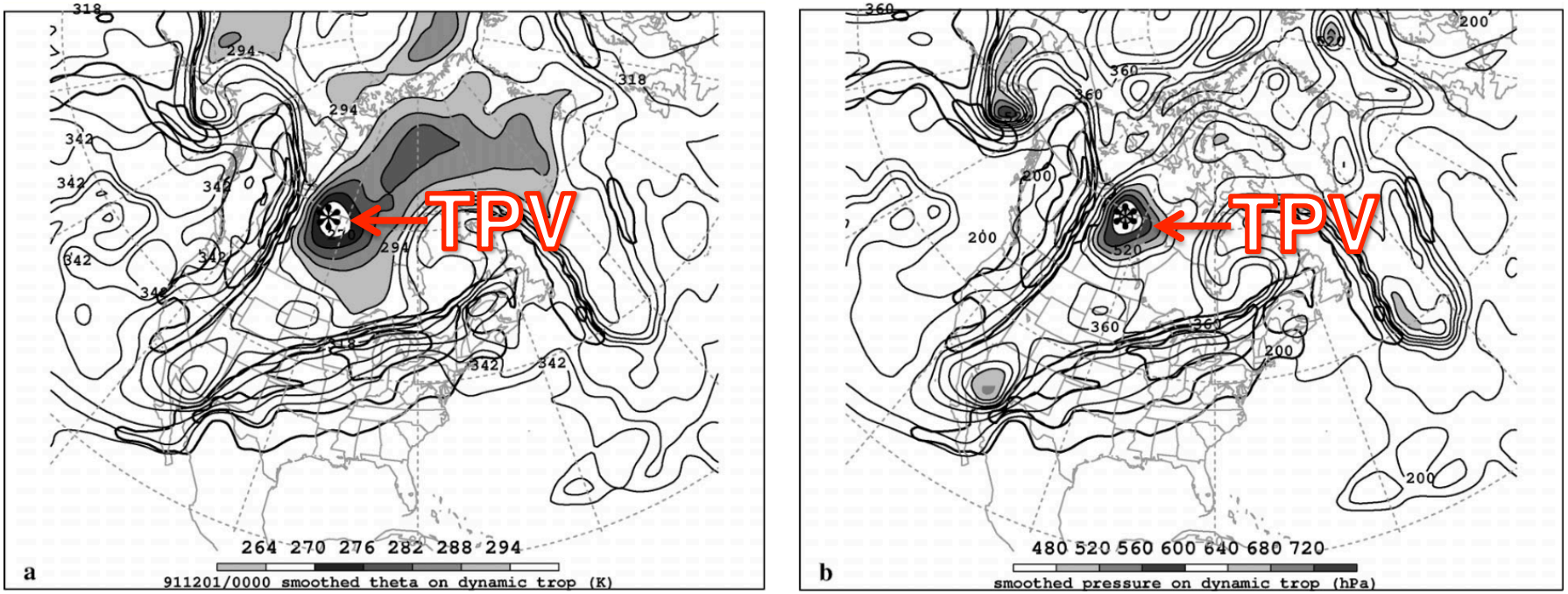

(left) Dynamic tropopause (DT) wind speed (every 15 m s^{-1} starting at 50 m s^{-1}, thick contours) and DT potential temperature (K, thin contours and shading) on 1.5-PVU surface valid 0000 UTC 1 Dec 1991; (right) same as left except DT pressure (hPa, thin contours and shading). Adapted from Fig. 11 in Pyle et al. (2004).

Motivation

- TPVs may interact with and strengthen midlatitude jet streams, and act as precursors to intense midlatitude cyclogenesis events
- Interactions between TPVs and midlatitude jet streams may lead to development of extreme weather events
- Surges of arctic air may accompany TPVs as they are transported to middle latitudes, resulting in widespread cold air outbreaks (CAOs)

Research Goals

- Increase understanding of the mechanisms responsible for the extraction of TPVs from high latitudes and their transport to middle latitudes

- Increase understanding of the relationship between TPVs and cold surges

Literature Review

- Past studies such as Hakim et al. (1995, 1996) and Bosart et al. (1996) have shown that ridge amplification may lead to the transport of TPVs to middle latitudes, where they may participate in the the development of intense midlatitude cyclones

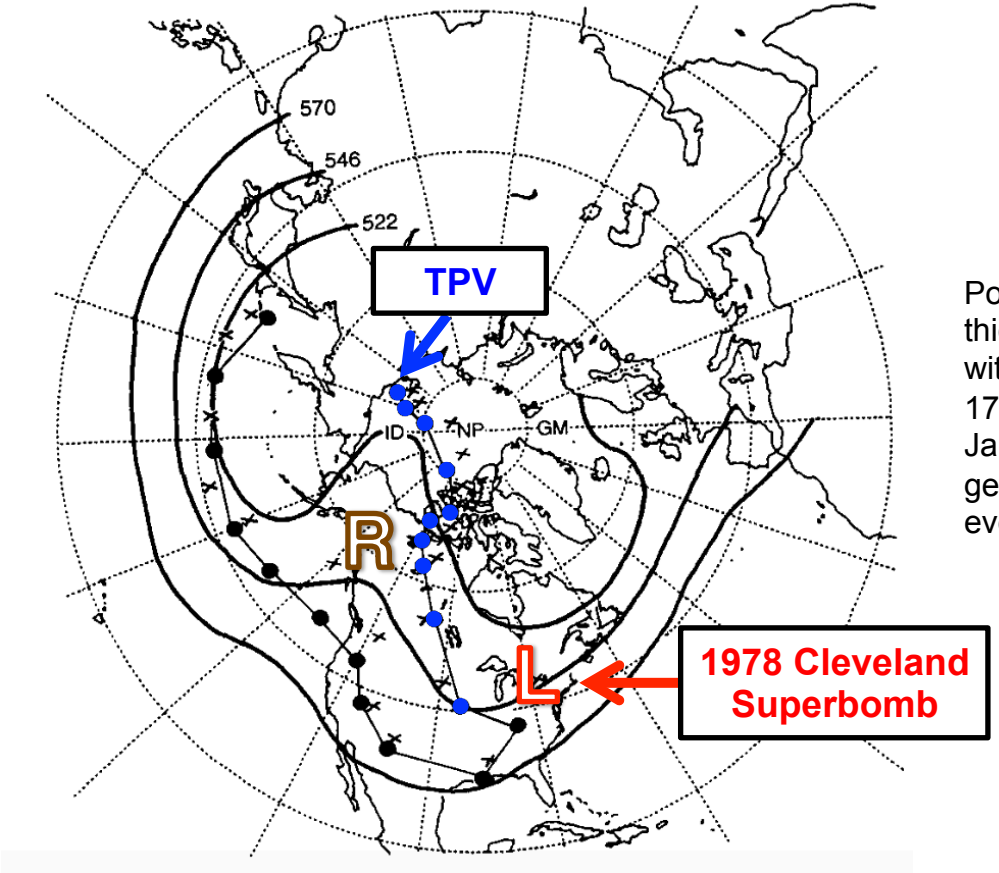

Position of QGPV maxima (colored dots) and thickness minima (black crosses) associated with CTDs every 24 h starting at 0000 UTC 17 January and ending 0000 UTC 27 January 1978; time-mean 500-hPa geopotential height field (black, contoured every 120 m) for 17–27 January 1978.

Adapted from Fig. 3 in Hakim et al. 1995

Literature Review

0000 UTC 20 Jan 1985

Adapted from Fig. 5 in Shapiro et al. (1987)

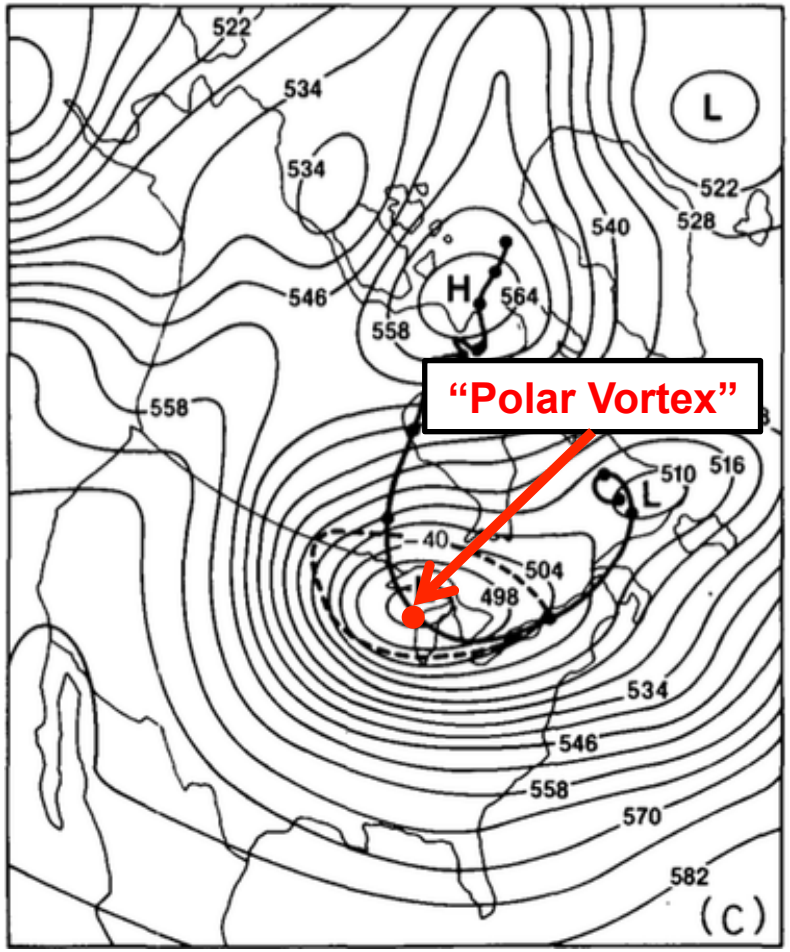

500-hPa geopotential height (black, every 6 dam) and −40°C isotherm (dashed contour); track of polar vortex from 0000 UTC 12 January to 0000 UTC 24 January 1985 (heavy black)

0.5° NCEP CFSR

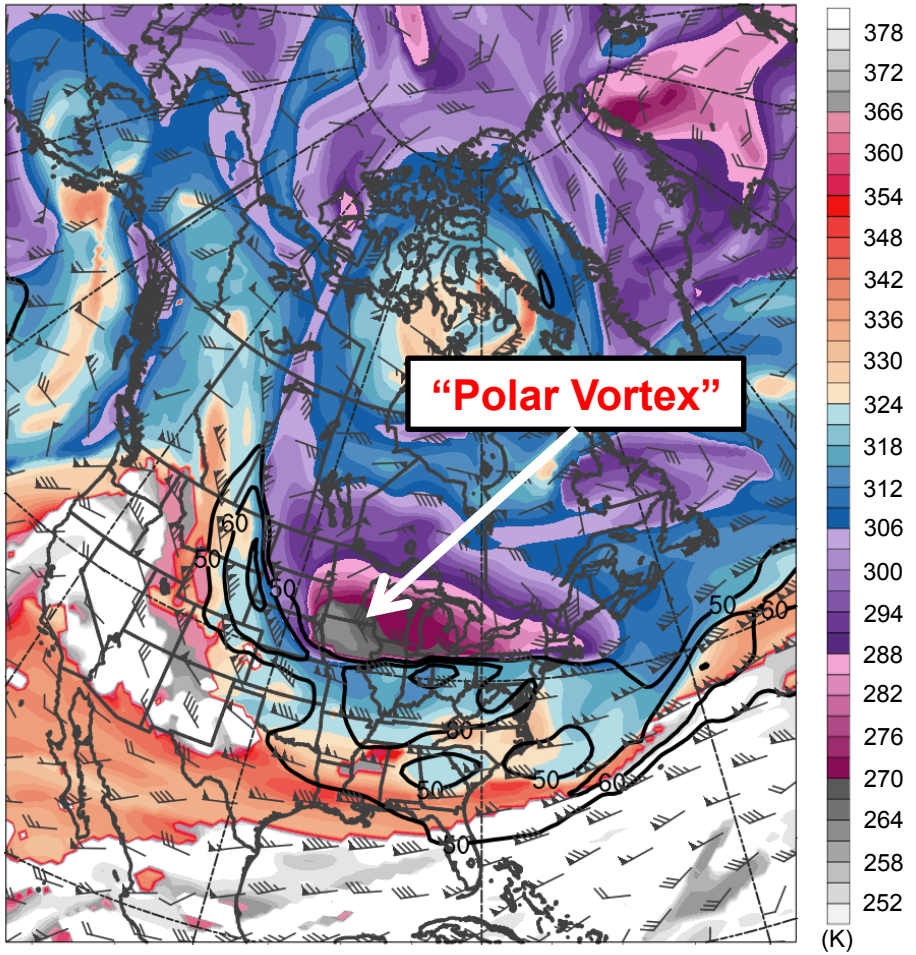

Potential temperature (K, shaded), wind speed (black, every 10 m s^{-1} starting at 50 m s^{-1}), and wind (m s^{-1}, barbs) on 2-PVU surface

Literature Review

0000 UTC 20 Jan 1985

- A commonality of cold air outbreaks (CAOs) over North America is surface anticyclogenesis occurring over northwestern North America prior to CAO onset (Colucci and Davenport 1987)

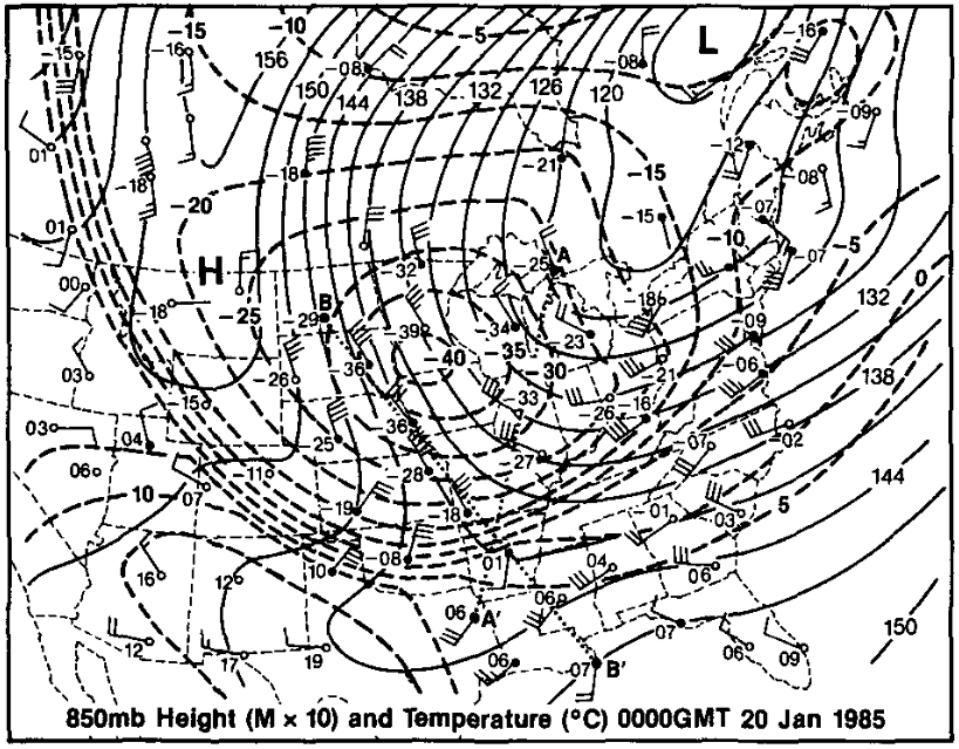

850-hPa geopotential height (solid, every 3 dam), temperature (dashed contour, every 5 K, and wind (barbs, m s^{-1}) at 0000 UTC 20 January 1985. Adapted from Fig. 8 in Shapiro et al. (1987).

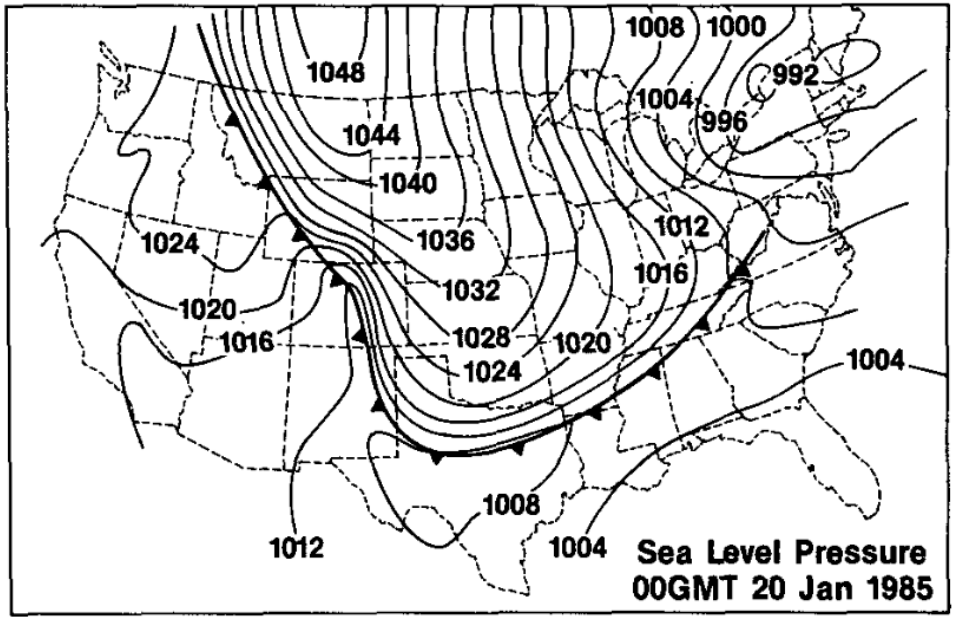

SLP (solid) and Arctic front (heavy spiked line) at 0000 UTC 20 January 1985. Adapted from Fig. 12 in Shapiro et al. (1987).

Literature Review

- Jones and Cohen (2011) composited 21 strong anticyclones (maximum MSLP ≥ 1050 hPa) occurring over northwestern North America from Nov–Mar of 1978/79 through 2001/02
- Anticyclogenesis occurs in region of strong forcing for descent downstream of a ridge, in left-entrance region of jet
- Cold air is advected equatorward east of the Rockies

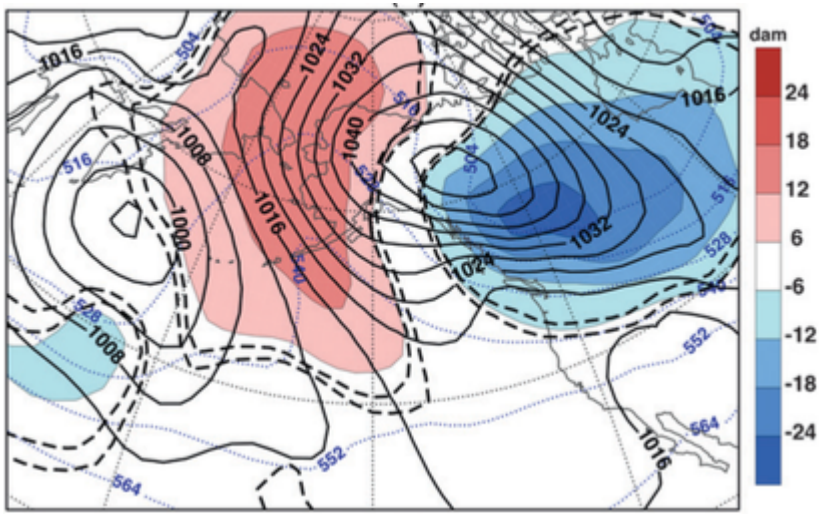

Composite SLP (hPa, solid black), 1000–500-hPa thickness (dam; dotted blue), thickness anomalies (shaded) at time of maximum SLP. Adapted from Fig. 4 in Jones and Cohen (2011)

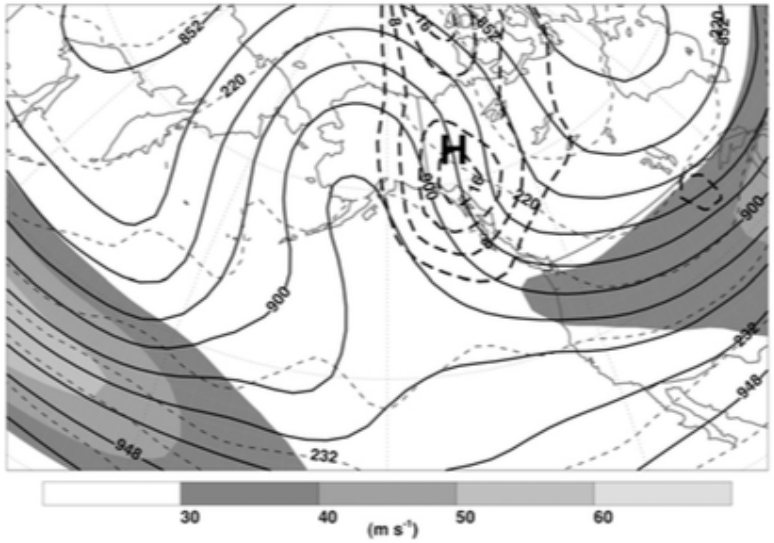

Composite 300-hPa geopotential heights (dam, solid black), wind speed (shaded, m s^{-1}), temperature (short dashes), and horizontal velocity convergence ($\times 10^{-6}$ s^{-1}, long dashes) at time of maximum SLP. Adapted from Fig. 3 in Jones and Cohen (2011)

Literature Review

- Pyle et al. (2004) has shown that the close approach of a TPV with a northerly flow jet over western North America resulted in jet intensification

- Could TPV interactions with jets lead to stronger secondary ageostrophic circulations, promoting increased subsidence, and contributing to stronger surface anticyclogenesis in the entrance region of these jets?

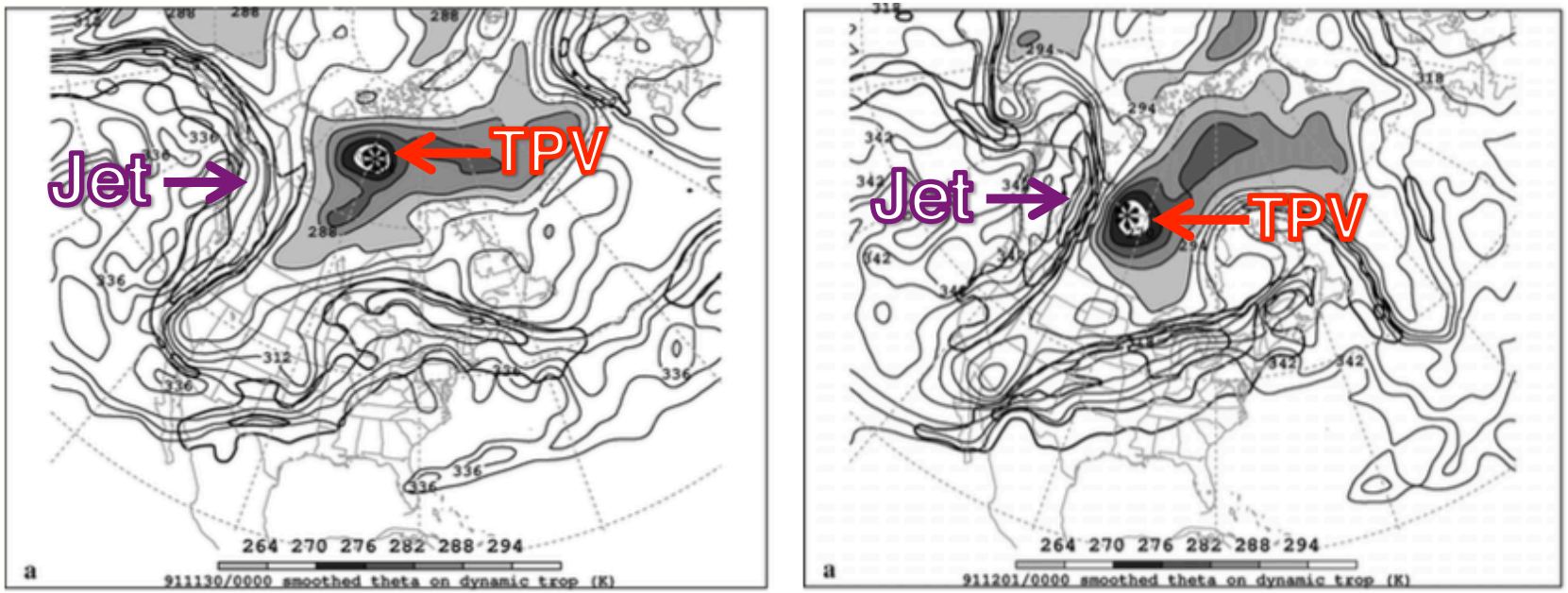

(left) DT (1.5-PVU surface) wind speed (every 15 m s^{-1} starting at 50 m s^{-1}, thick contours) and potential temperature (K, thin contours and shading) at 0000 UTC 30 Nov 1991; (right) same as left except 0000 UTC 1 Dec 1991

Hypotheses

- The northerly flow found just downstream of amplifying ridges supports the extraction of TPVs from high latitudes and their transport into middle latitudes

- Disturbances such as extratropical cyclones and transitioning and recurving tropical cyclones may play important roles in leading to these amplifying ridges

- TPVs may serve as catalysts for CAOs as artic air found beneath and behind TPVs surge equatorward when TPVs are transported into middle latitudes

- TPVs interactions with jets on the downstream side of ridges may lead to strengthening of these jets, supporting stronger forcing for descent and thus stronger surface anticyclogenesis in the entrance region

Methodology

- Perform multi-scale case study investigations of two TPVs associated with CAOs using 0.5° NCEP CFSR dataset (Saha et al. 2010)
  - **Case 1:** 9–11 January 1982 CAO over central and eastern North America
  - **Case 2:** 13–14 February 2016 CAO over eastern North America
- Both events resulted in minimum temperature records across portions of North America

Methodology

- Subjective TPV identification and tracking
  - TPV must be a coherent vortex that exhibits a local minimum of DT θ (i.e., closed contours of DT θ) on 2 PVU surface
  - The vortex must be of high-latitude origin and last ≥ 2 days, similar to Cavallo and Hakim (2009)
  - Stop tracking TPV when it becomes significantly deformed during interaction with NAJ

Methodology

- Diagnose QG forcing for vertical motion as TPV approaches and/or interacts with northerly flow jet located on downstream side of upstream ridge in each case

- Q-vectors in pressure coordinates calculated following Hoskins and Pedder (1980):

$$\boldsymbol{Q} = -\left(\frac{\partial \mathbf{v}_g}{\partial x} \cdot \nabla_p \theta\right) \boldsymbol{i} - \left(\frac{\partial \mathbf{v}_g}{\partial y} \cdot \nabla_p \theta\right) \boldsymbol{j}$$

- Q-vectors separated into along-isentrope ($\mathbf{Q}_s$) and across-isentrope ($\mathbf{Q}_n$) components following Keyser et al. (1992) as follows:

$$\boldsymbol{Q}_s = \left(\frac{\boldsymbol{Q} \cdot (\boldsymbol{k} \times \nabla\theta)}{|\nabla\theta|}\right) \frac{\boldsymbol{k} \times \nabla\theta}{|\nabla\theta|}$$

$$\boldsymbol{Q}_n = \left[\boldsymbol{Q} \cdot \left(-\frac{\nabla\theta}{|\nabla\theta|}\right)\right] \left(-\frac{\nabla\theta}{|\nabla\theta|}\right)$$

Methodology

- QG forcing for $\mathbf{Q}_s$ and $\mathbf{Q}_n$ calculated by adapting Q-vector form of omega equation in pressure coordinates from Hoskins and Pedder (1980)

$$\left(\sigma\nabla_p^2 + f_0^2\frac{\partial^2}{\partial p^2}\right)\omega = -2h\left(\nabla_p \cdot \boldsymbol{Q}_s\right)$$

$$\left(\sigma\nabla_p^2 + f_0^2\frac{\partial^2}{\partial p^2}\right)\omega = -2h\left(\nabla_p \cdot \boldsymbol{Q}_n\right)$$

where $h = (\rho\,\theta)^{-1}$, or equivalently, $h = \frac{R}{p_o}\left(\frac{p_0}{p}\right)^{c_v/c_p}$

- Q-vector components and respective forcings for vertical motion averaged over 600–400-hPa layer

TPV 1 Track: 1800 UTC 11 Dec 1981 – 0000 UTC 11 Jan 1982

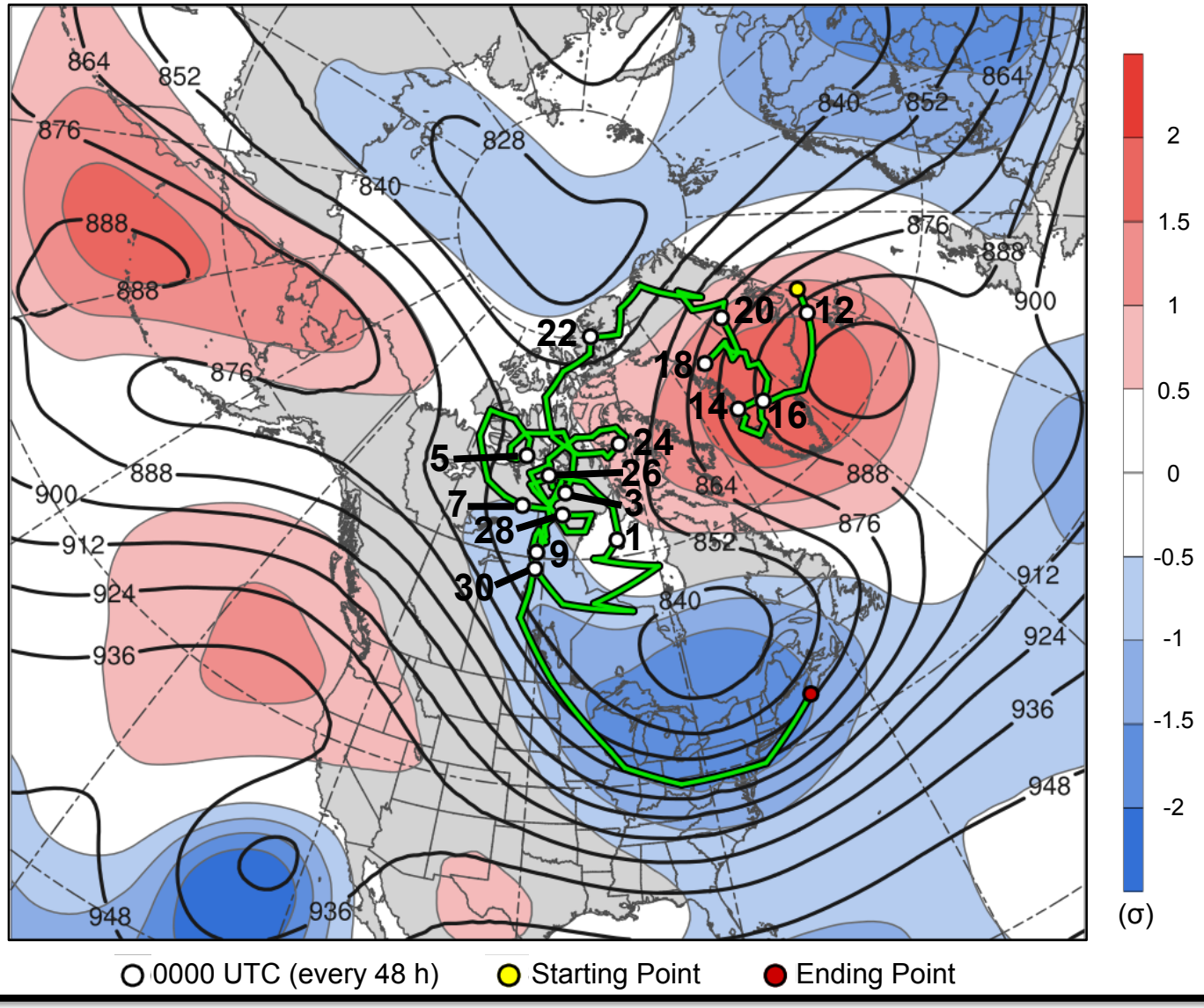

7–11 January 1982 time-mean 300-hPa geopotential height (dam, black) and standardized anomaly of geopotential height (σ, shaded)

Case 1: Upstream Ridge Evolution

0000 UTC 6 Jan 1982

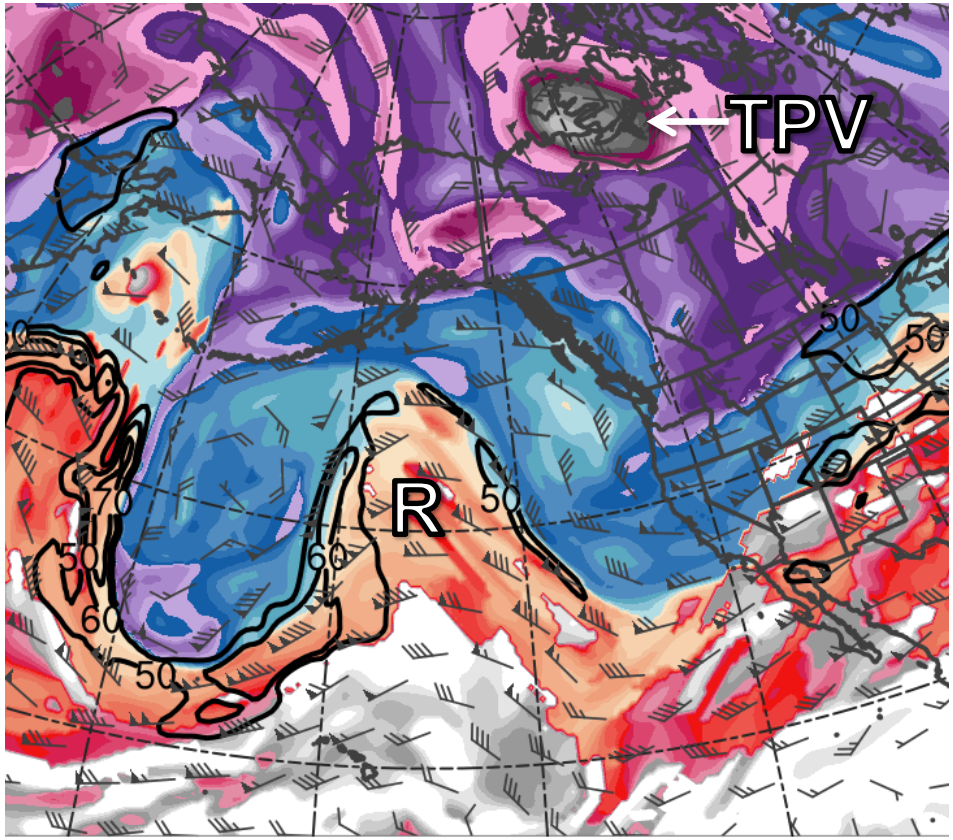

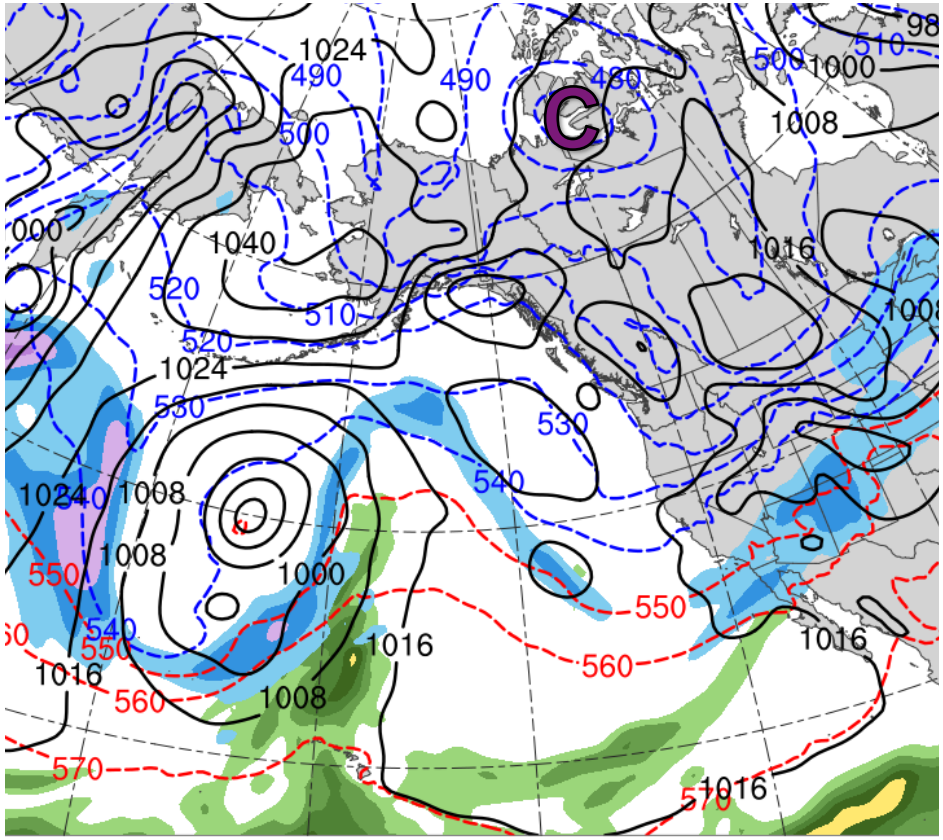

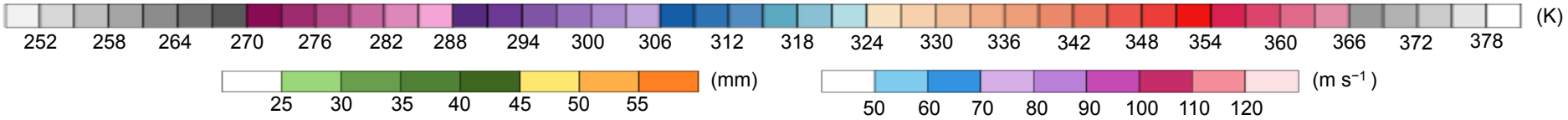

Potential temperature (K, shaded), wind speed (black, every 10 m s^{-1} starting at 50 m s^{-1}), and wind (m s^{-1}, barbs) on 2-PVU surface

250-hPa wind speed (m s^{-1}, shaded), 1000–500-hPa thickness (every 10 dam, blue/red), MSLP (every 8 hPa, black), PW (mm, shaded)

Case 1: Upstream Ridge Evolution

1200 UTC 7 Jan 1982

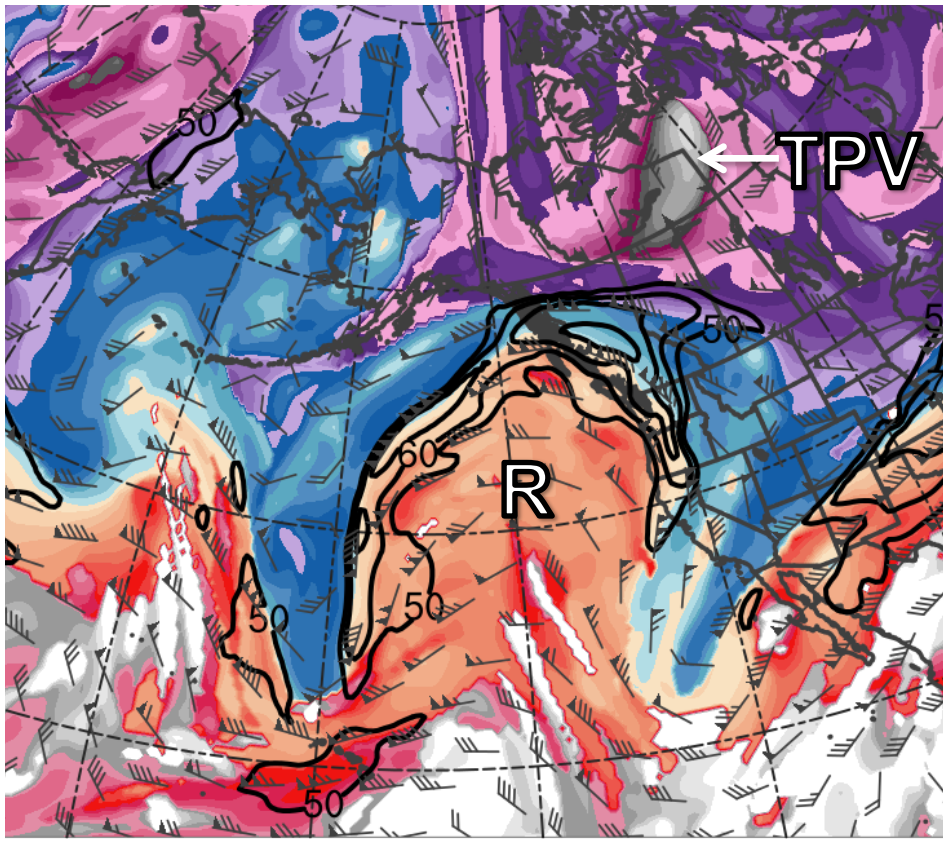

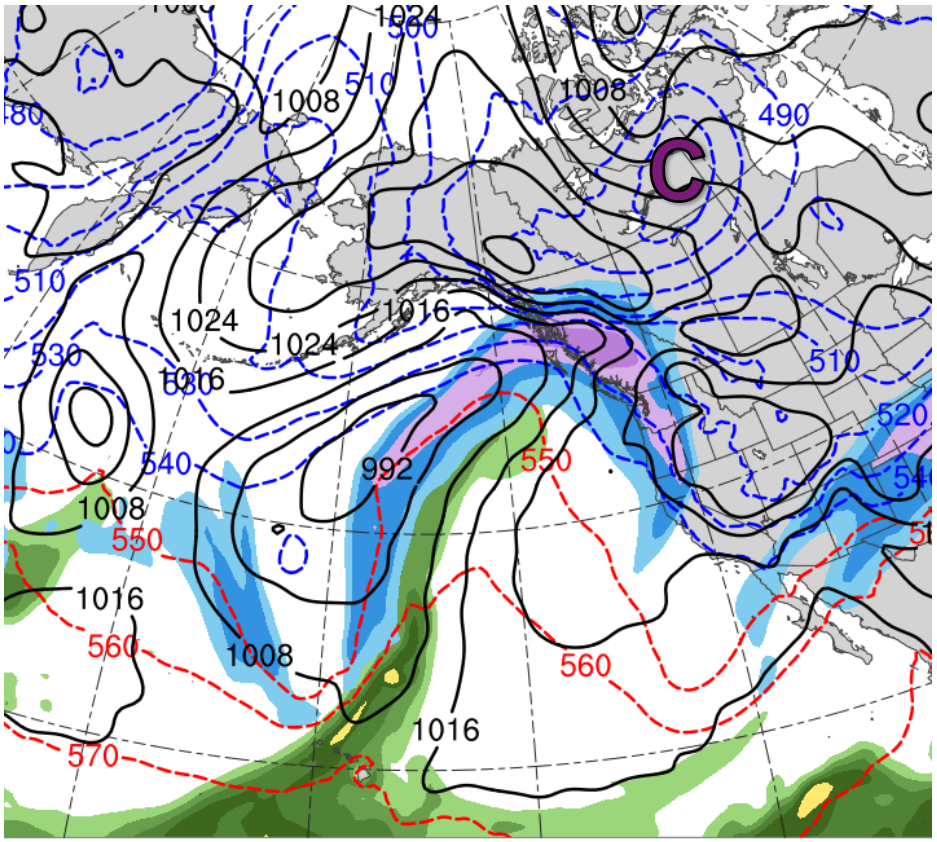

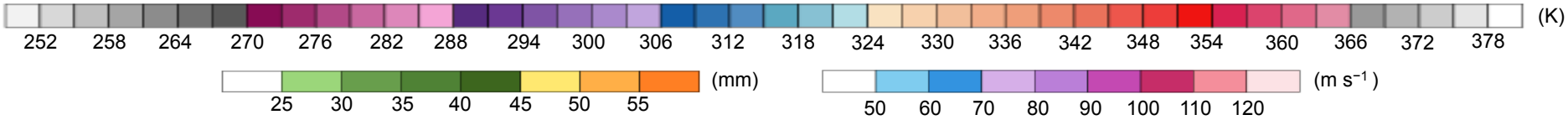

Potential temperature (K, shaded), wind speed (black, every 10 m s^{-1} starting at 50 m s^{-1}), and wind (m s^{-1}, barbs) on 2-PVU surface

250-hPa wind speed (m s^{-1}, shaded), 1000–500-hPa thickness (every 10 dam, blue/red), MSLP (every 8 hPa, black), PW (mm, shaded)

Case 1: Upstream Ridge Evolution

0000 UTC 9 Jan 1982

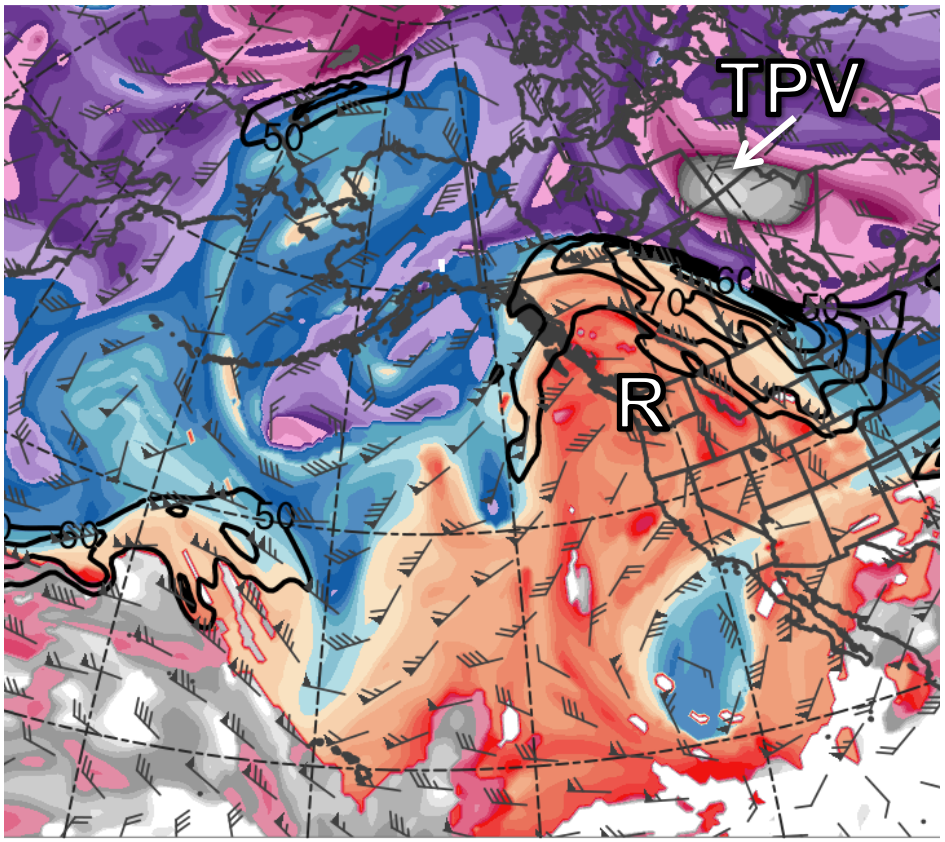

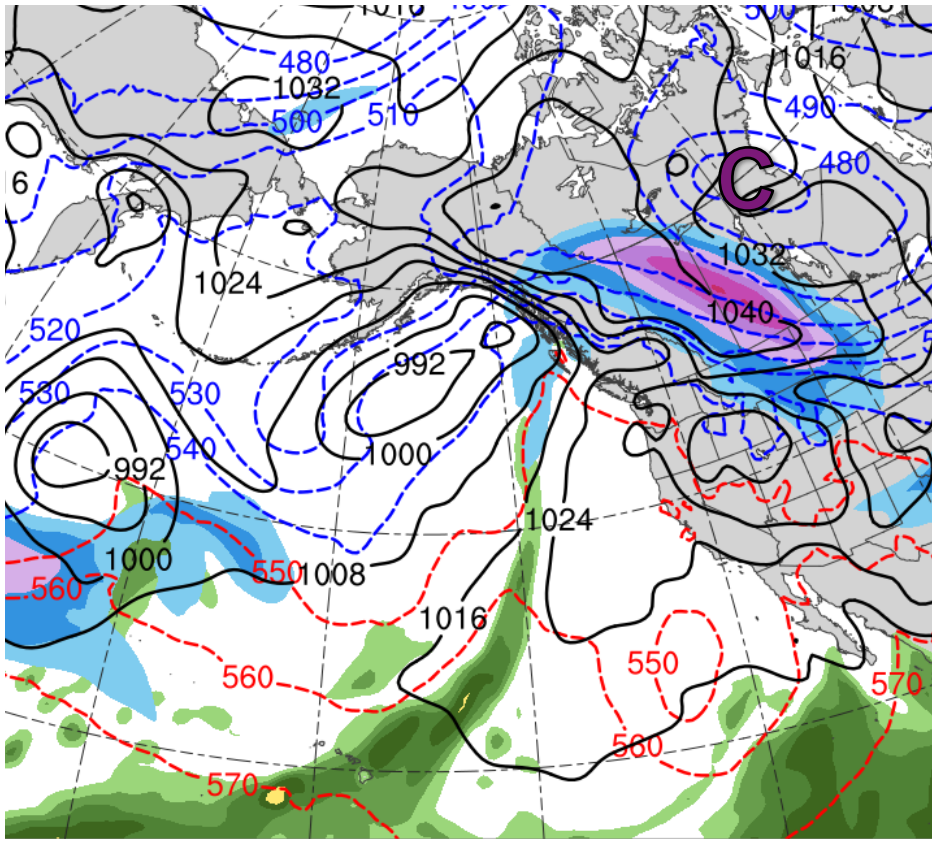

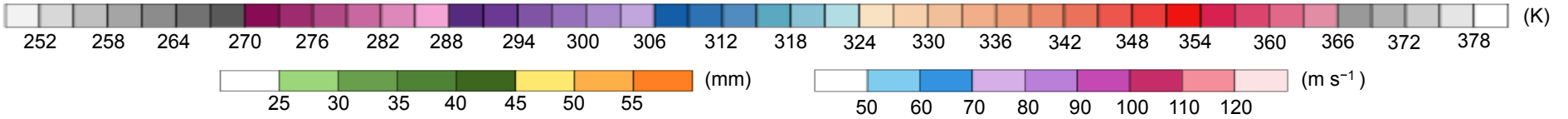

Potential temperature (K, shaded), wind speed (black, every 10 m s^{-1} starting at 50 m s^{-1}), and wind (m s^{-1}, barbs) on 2-PVU surface

250-hPa wind speed (m s^{-1}, shaded), 1000–500-hPa thickness (every 10 dam, blue/red), MSLP (every 8 hPa, black), PW (mm, shaded)

Case 1: TPV Transport and CAO

1200 UTC 8 Jan 1982

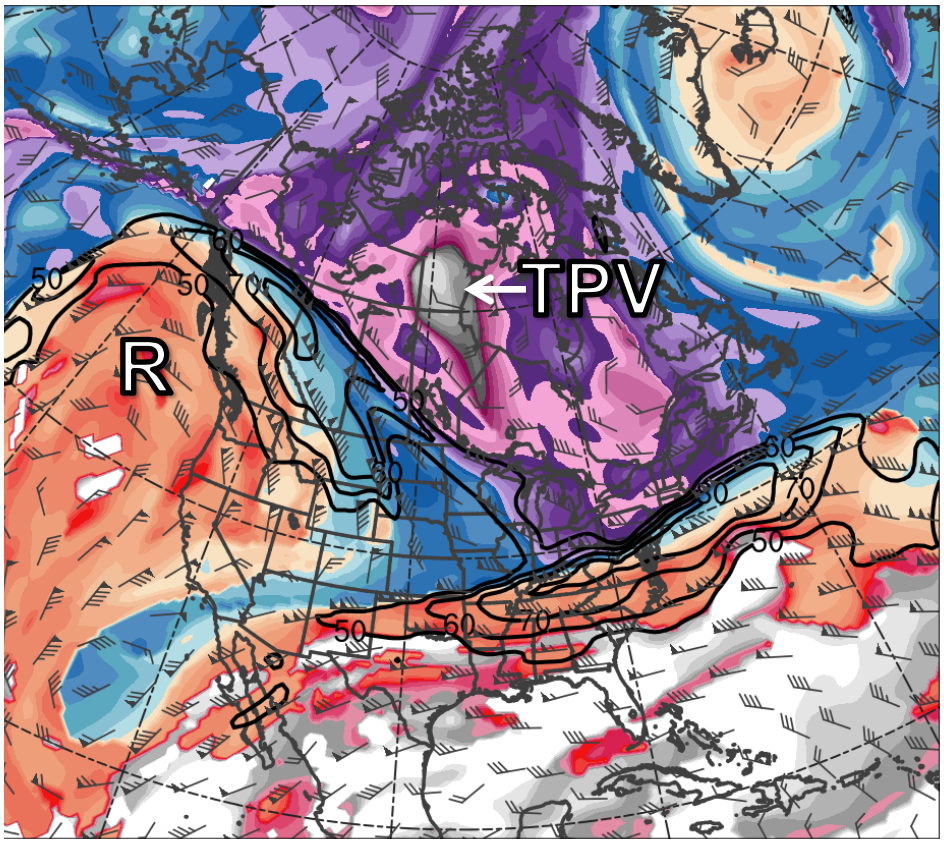

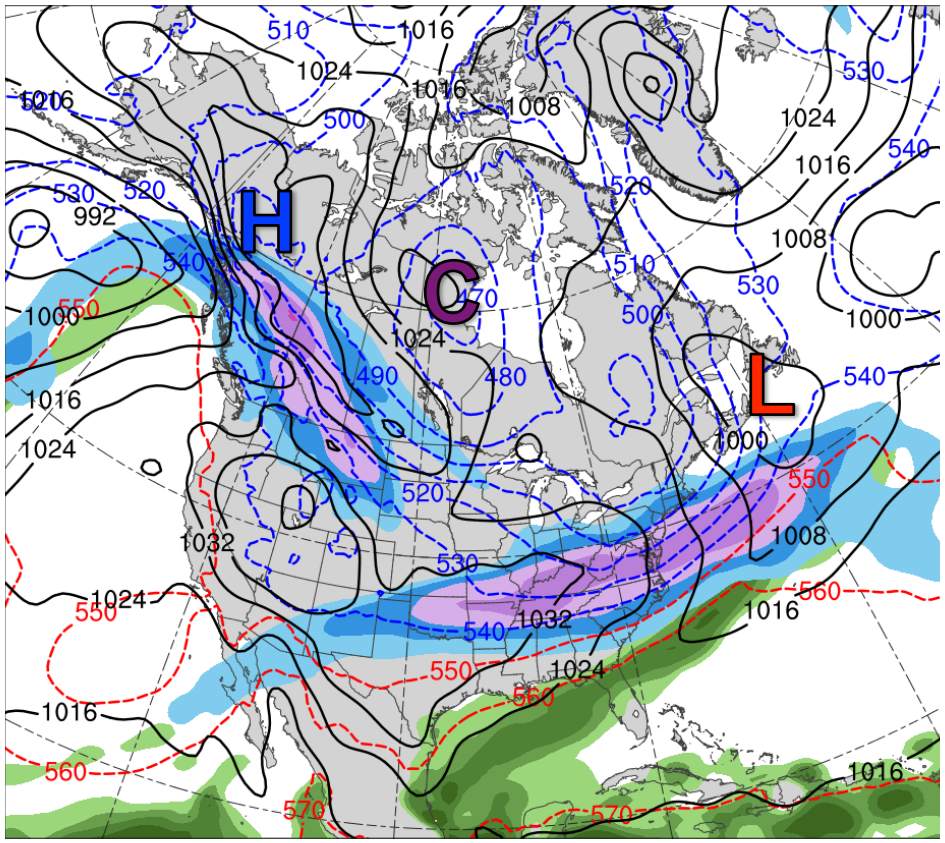

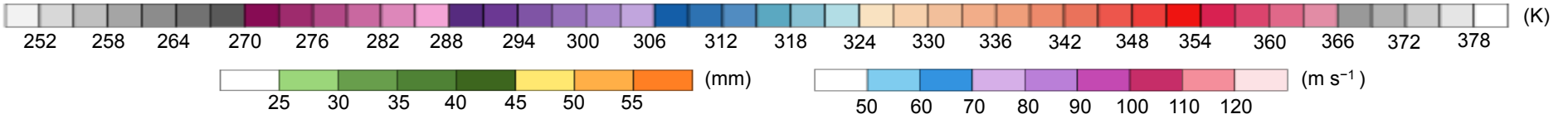

Potential temperature (K, shaded), wind speed (black, every 10 m s^{-1} starting at 50 m s^{-1}), and wind (m s^{-1}, barbs) on 2-PVU surface

250-hPa wind speed (m s^{-1}, shaded), 1000–500-hPa thickness (every 10 dam, blue/red), MSLP (every 8 hPa, black), PW (mm, shaded)

Case 1: TPV Transport and CAO

1200 UTC 9 Jan 1982

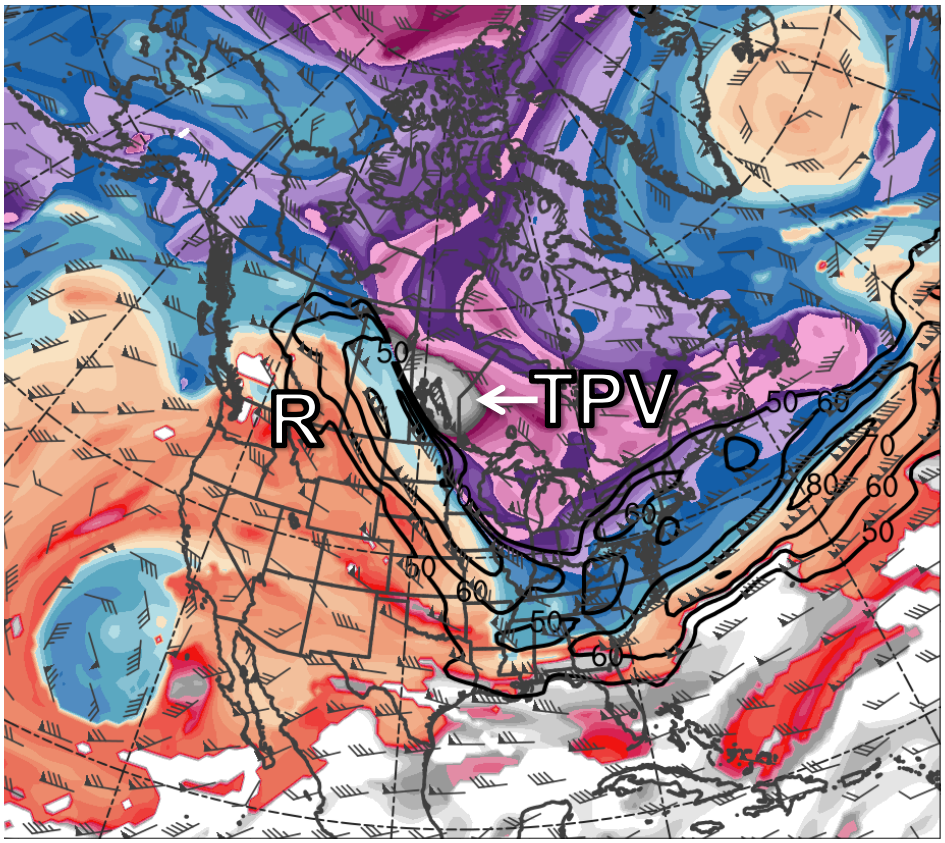

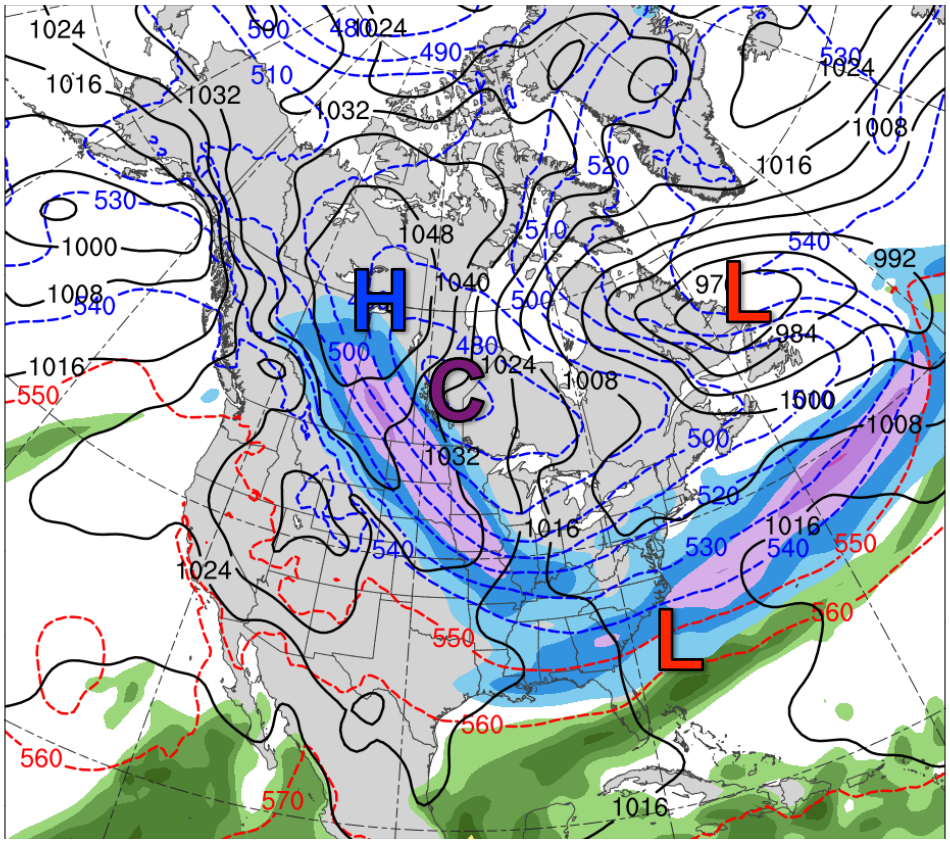

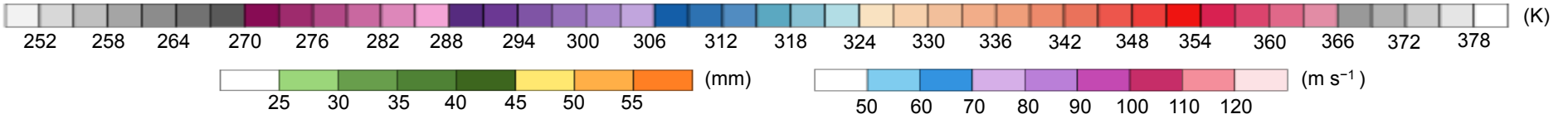

Potential temperature (K, shaded), wind speed (black, every 10 m s^{-1} starting at 50 m s^{-1}), and wind (m s^{-1}, barbs) on 2-PVU surface

250-hPa wind speed (m s^{-1}, shaded), 1000–500-hPa thickness (every 10 dam, blue/red), MSLP (every 8 hPa, black), PW (mm, shaded)

Case 1: TPV Transport and CAO

1200 UTC 10 Jan 1982

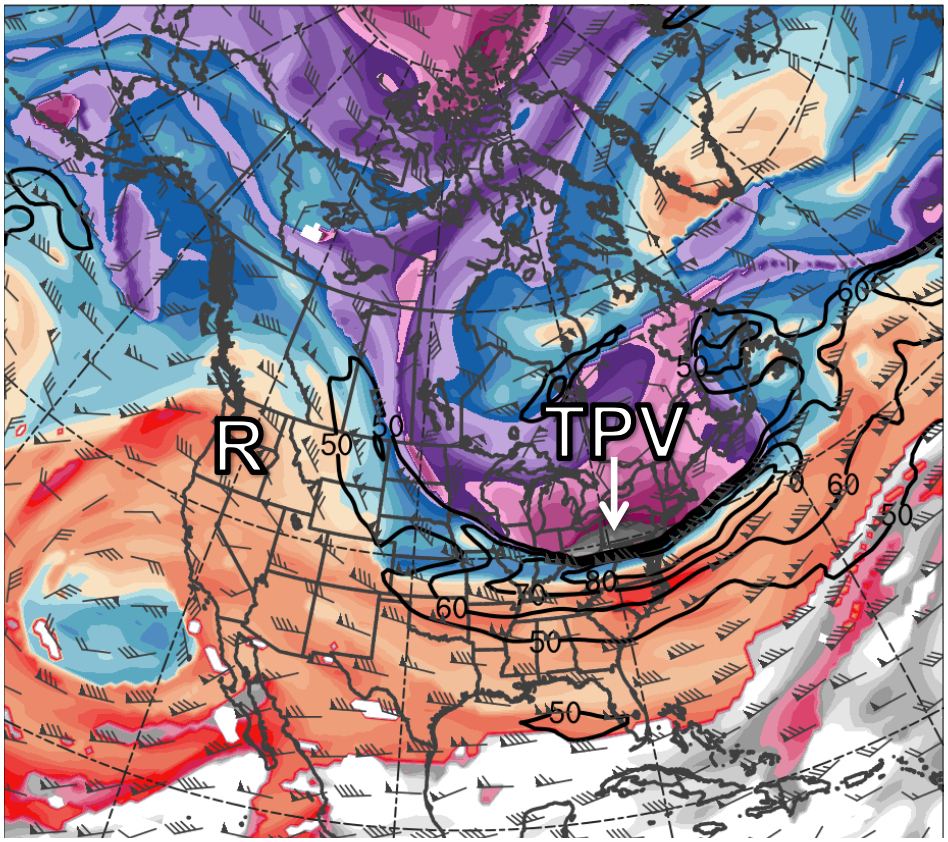

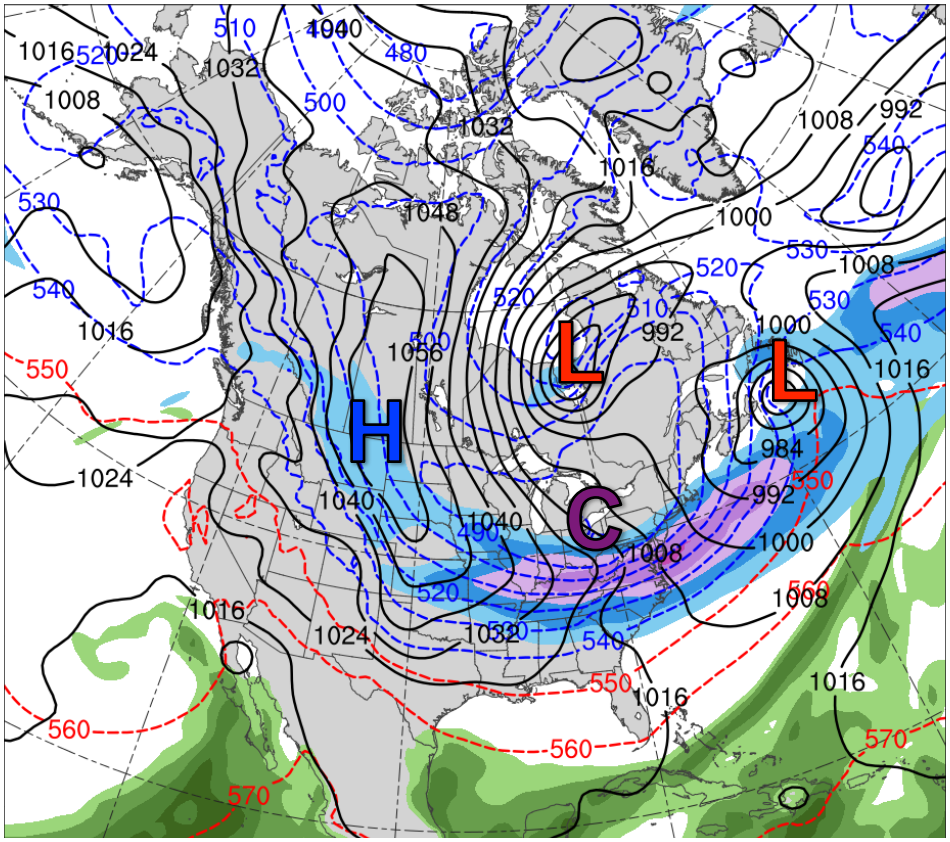

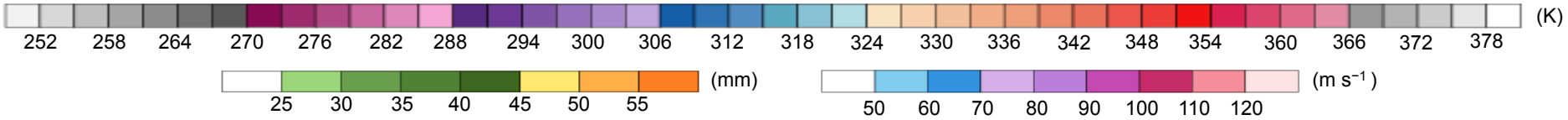

Potential temperature (K, shaded), wind speed (black, every 10 m s^{-1} starting at 50 m s^{-1}), and wind (m s^{-1}, barbs) on 2-PVU surface

250-hPa wind speed (m s^{-1}, shaded), 1000–500-hPa thickness (every 10 dam, blue/red), MSLP (every 8 hPa, black), PW (mm, shaded)

Case 1: Cross Section

1800 UTC 9 Jan 1982

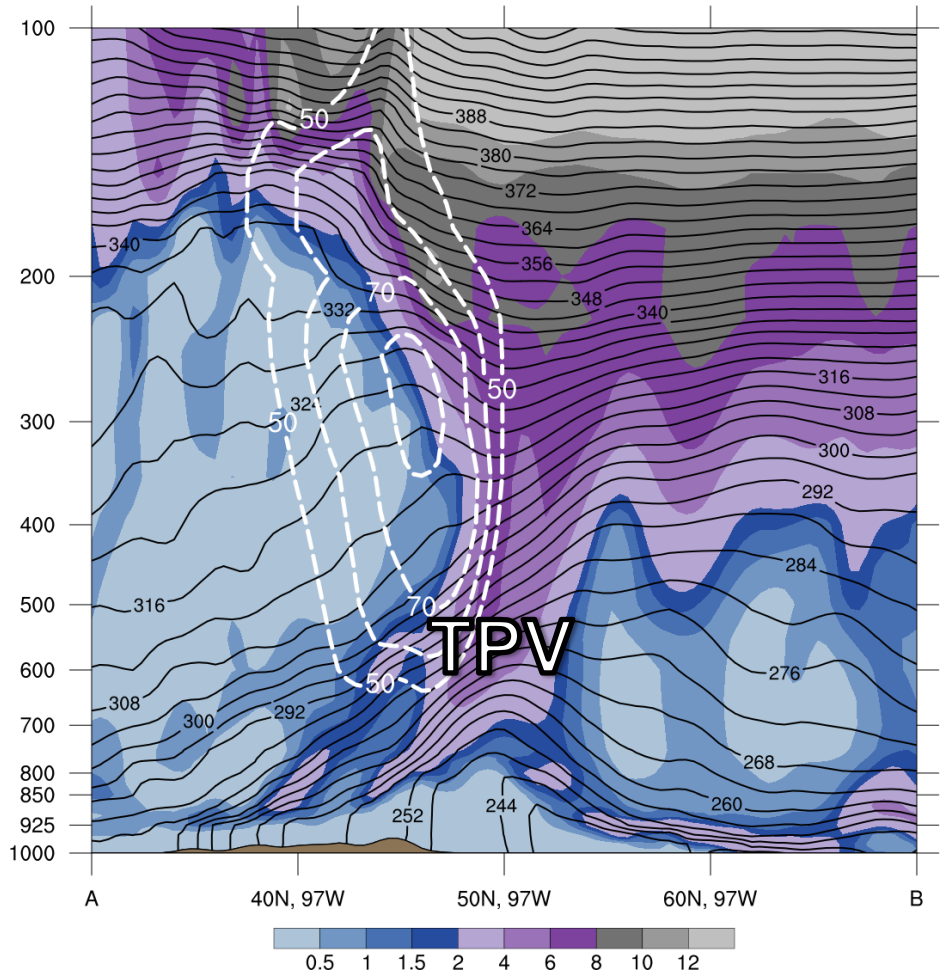

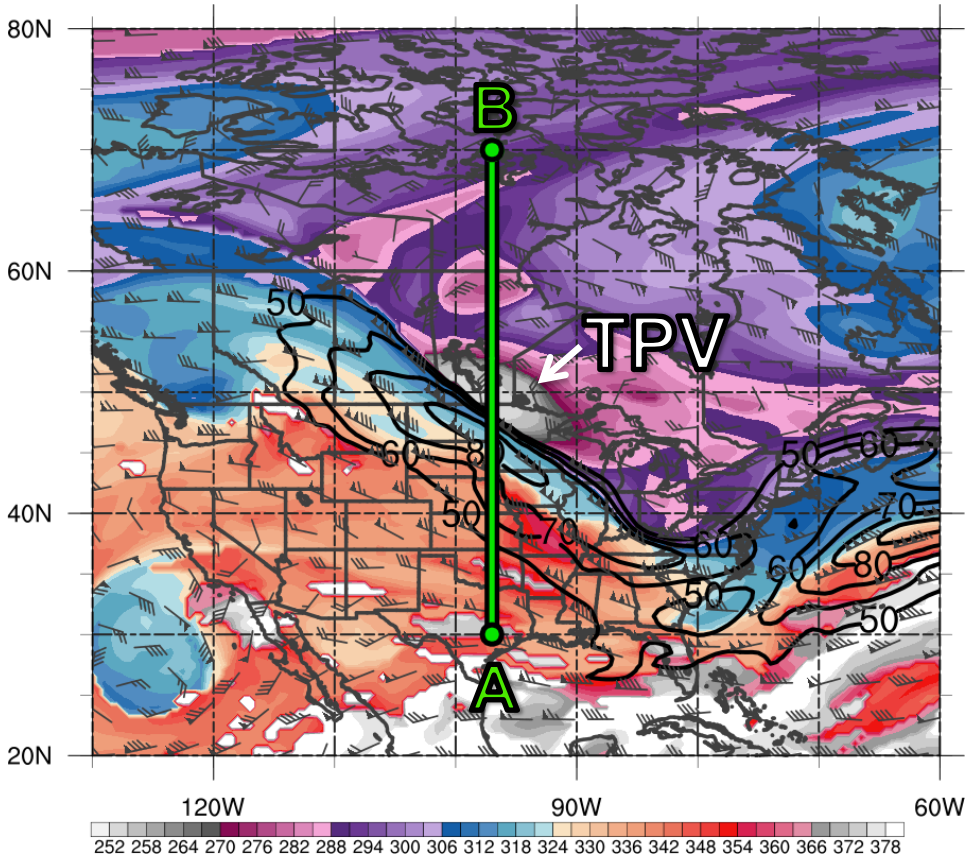

Potential vorticity (PVU, shaded), wind speed (white, every 10 m s^{-1} starting at 50 m s^{-1}), and potential temperature (K, black)

Potential temperature (K, shaded), wind speed (black, every 10 m s^{-1} starting at 50 m s^{-1}), and wind (m s^{-1}, barbs) on 2-PVU surface

Case 1: QG Diagnostics

0600 UTC 9 Jan 1982

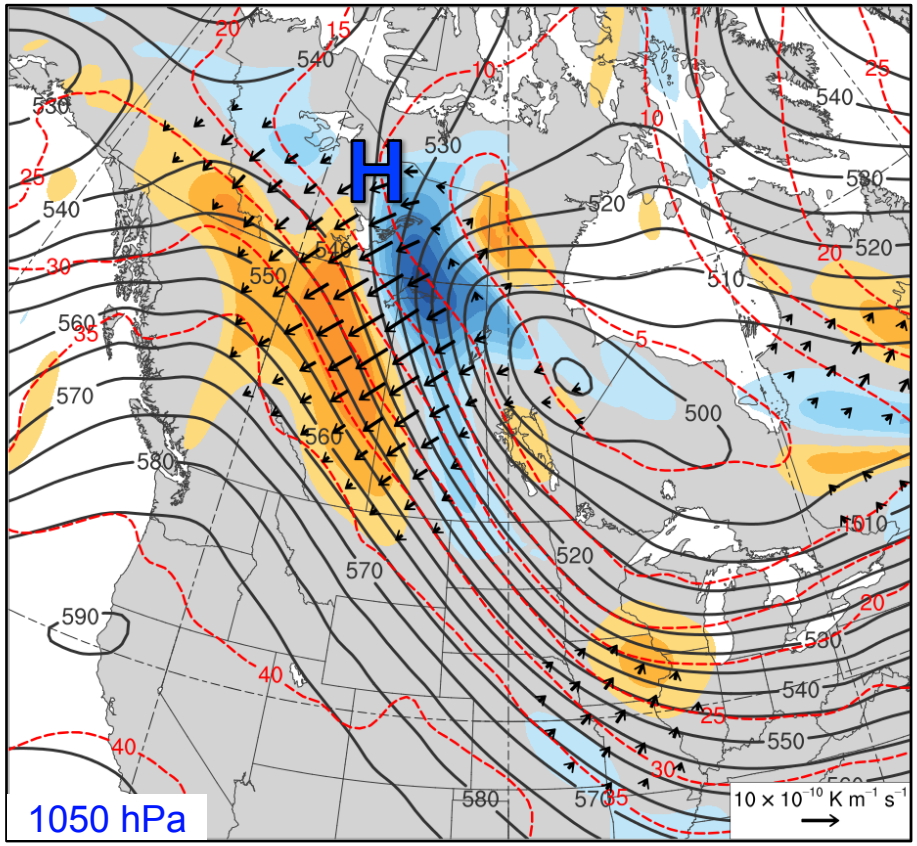

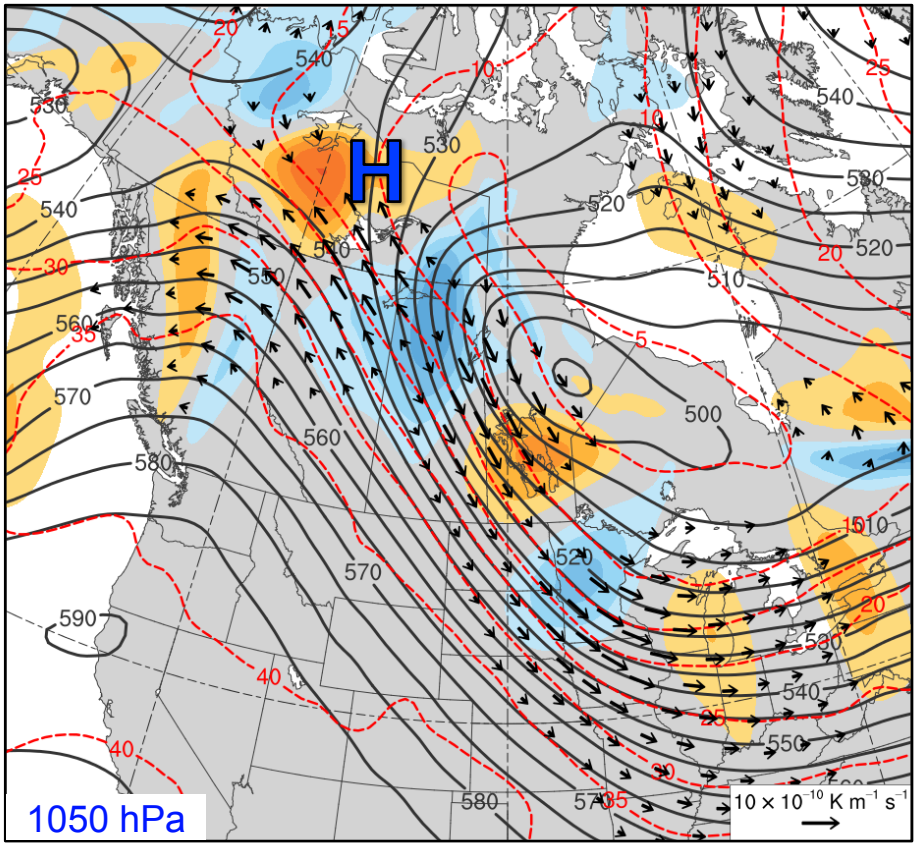

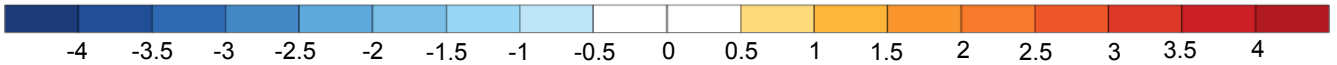

600–400-hPa layer averaged $\mathbf{Q}_n$ (K m^{-1} s^{-1}, vectors), $\mathbf{Q}_n$ forcing for vertical motion (×10^{-18} Pa^{-1} s^{-3}, shaded), geopotential height (dam, gray), and potential temperature (K, red)

600–400-hPa layer averaged $\mathbf{Q}_s$ (K m^{-1} s^{-1}, vectors), $\mathbf{Q}_s$ forcing for vertical motion (×10^{-18} Pa^{-1} s^{-3}, shaded), geopotential height (dam, gray), and potential temperature (K, red)

Case 1: QG Diagnostics

1200 UTC 9 Jan 1982

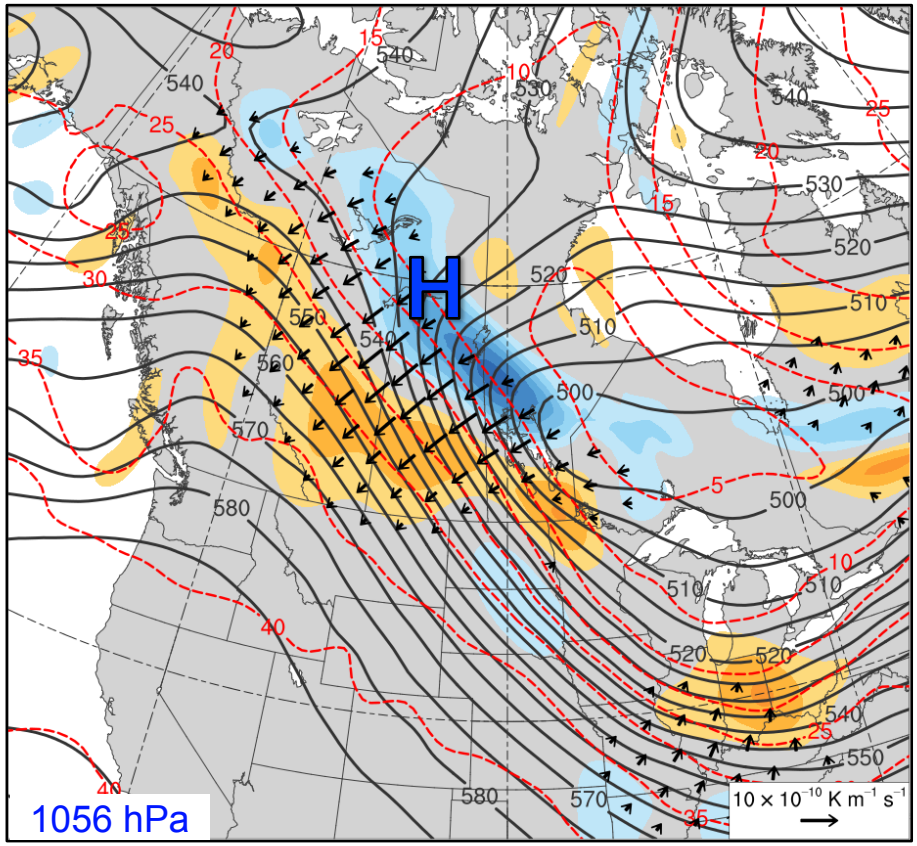

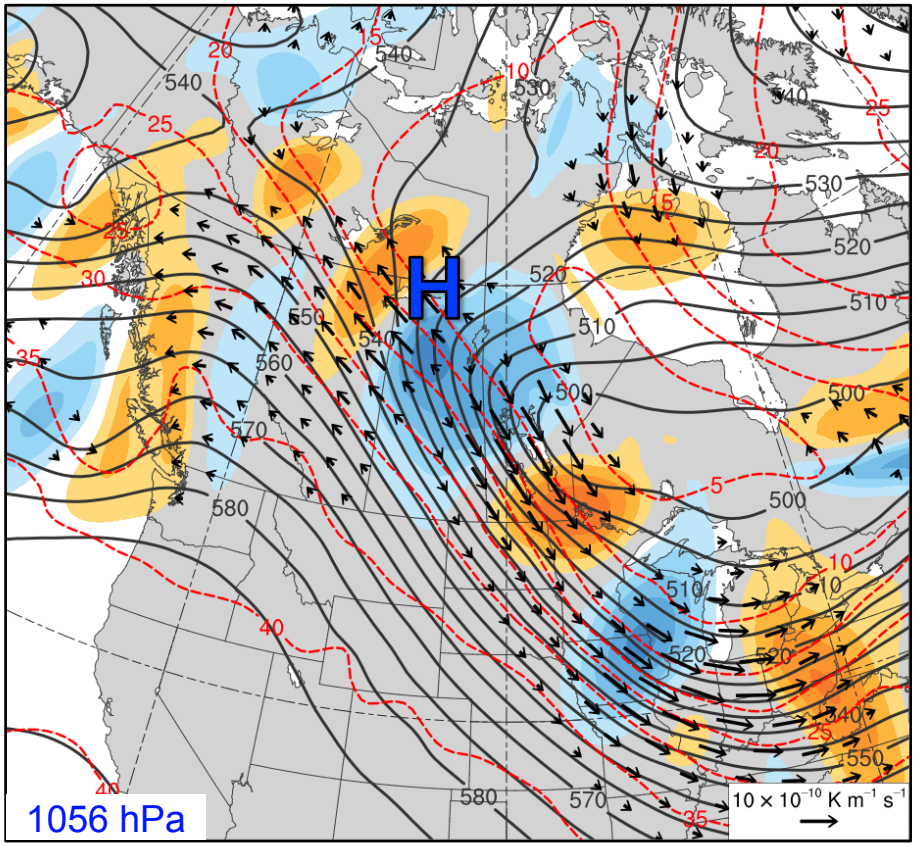

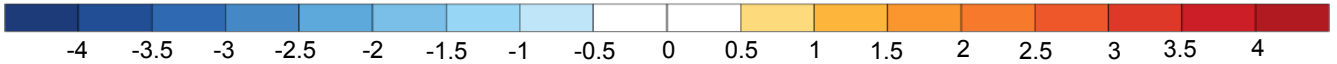

600–400-hPa layer averaged $\mathbf{Q}_n$ (K m^{-1} s^{-1}, vectors), $\mathbf{Q}_n$ forcing for vertical motion (×10^{-18} Pa^{-1} s^{-3}, shaded), geopotential height (dam, gray), and potential temperature (K, red)

600–400-hPa layer averaged $\mathbf{Q}_s$ (K m^{-1} s^{-1}, vectors), $\mathbf{Q}_s$ forcing for vertical motion (×10^{-18} Pa^{-1} s^{-3}, shaded), geopotential height (dam, gray), and potential temperature (K, red)

Case 1: QG Diagnostics

1200 UTC 9 Jan 1982

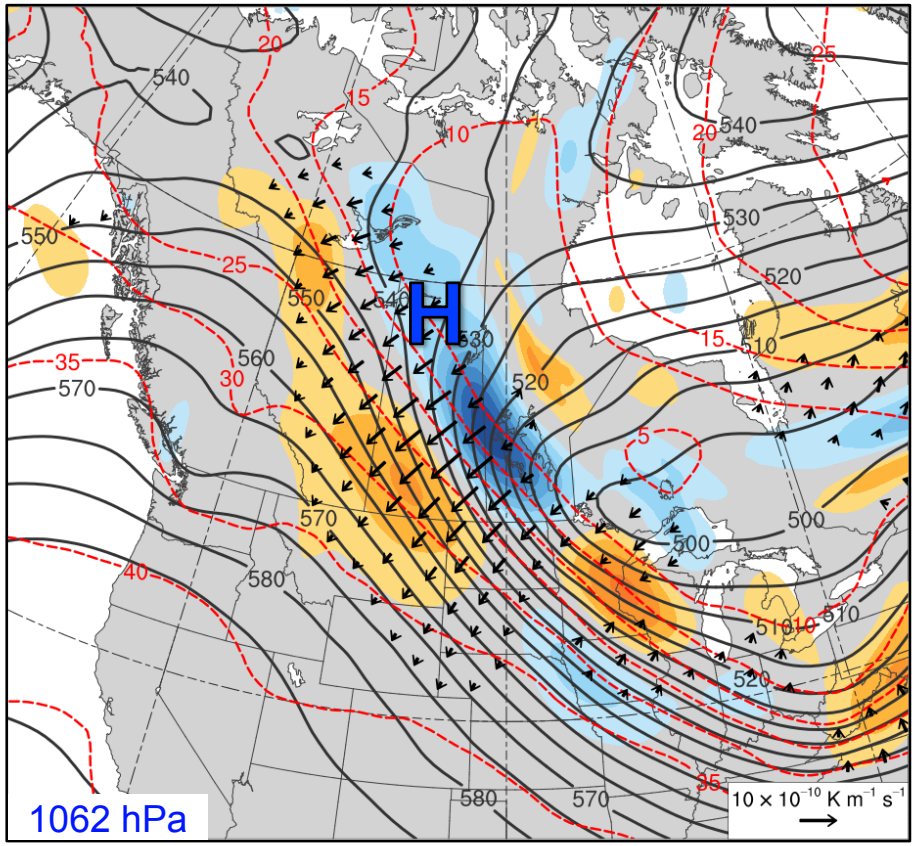

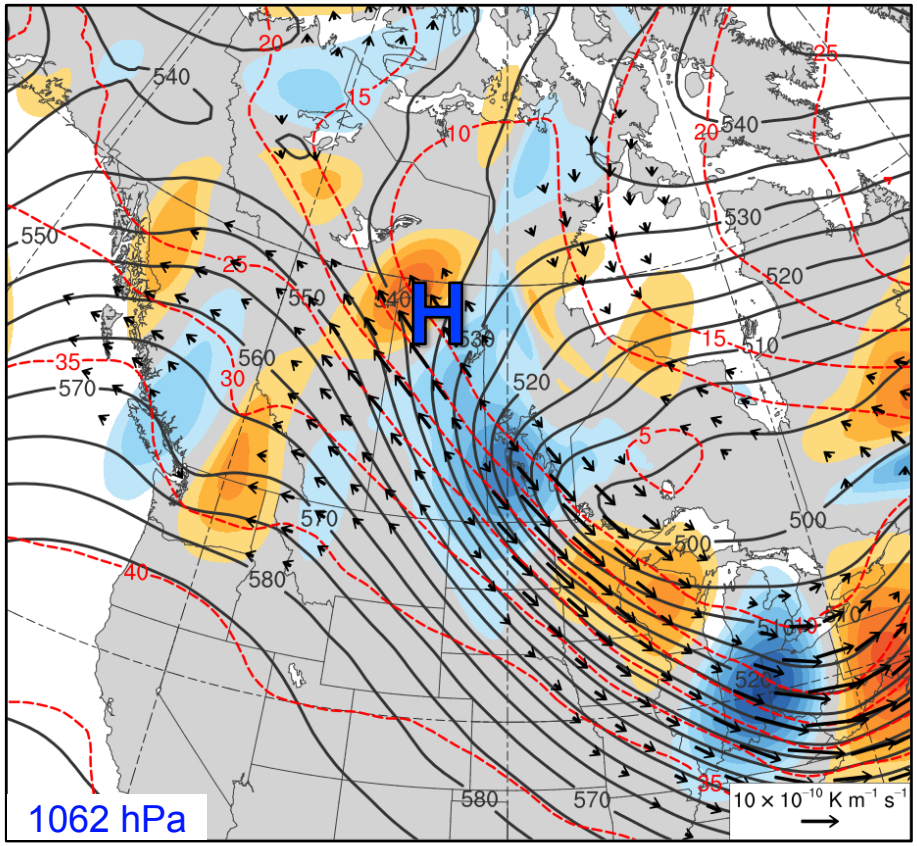

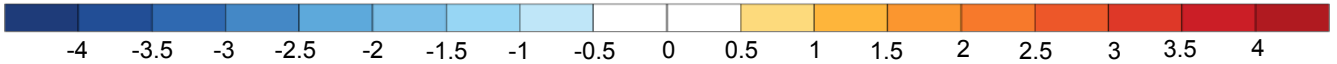

600–400-hPa layer averaged $\mathbf{Q}_n$ (K m^{-1} s^{-1}, vectors), $\mathbf{Q}_n$ forcing for vertical motion (×10^{-18} Pa^{-1} s^{-3}, shaded), geopotential height (dam, gray), and potential temperature (K, red)

600–400-hPa layer averaged $\mathbf{Q}_s$ (K m^{-1} s^{-1}, vectors), $\mathbf{Q}_s$ forcing for vertical motion (×10^{-18} Pa^{-1} s^{-3}, shaded), geopotential height (dam, gray), and potential temperature (K, red)

TPV 2 Track: 1800 UTC 6 Feb – 1800 UTC 14 Feb 2016

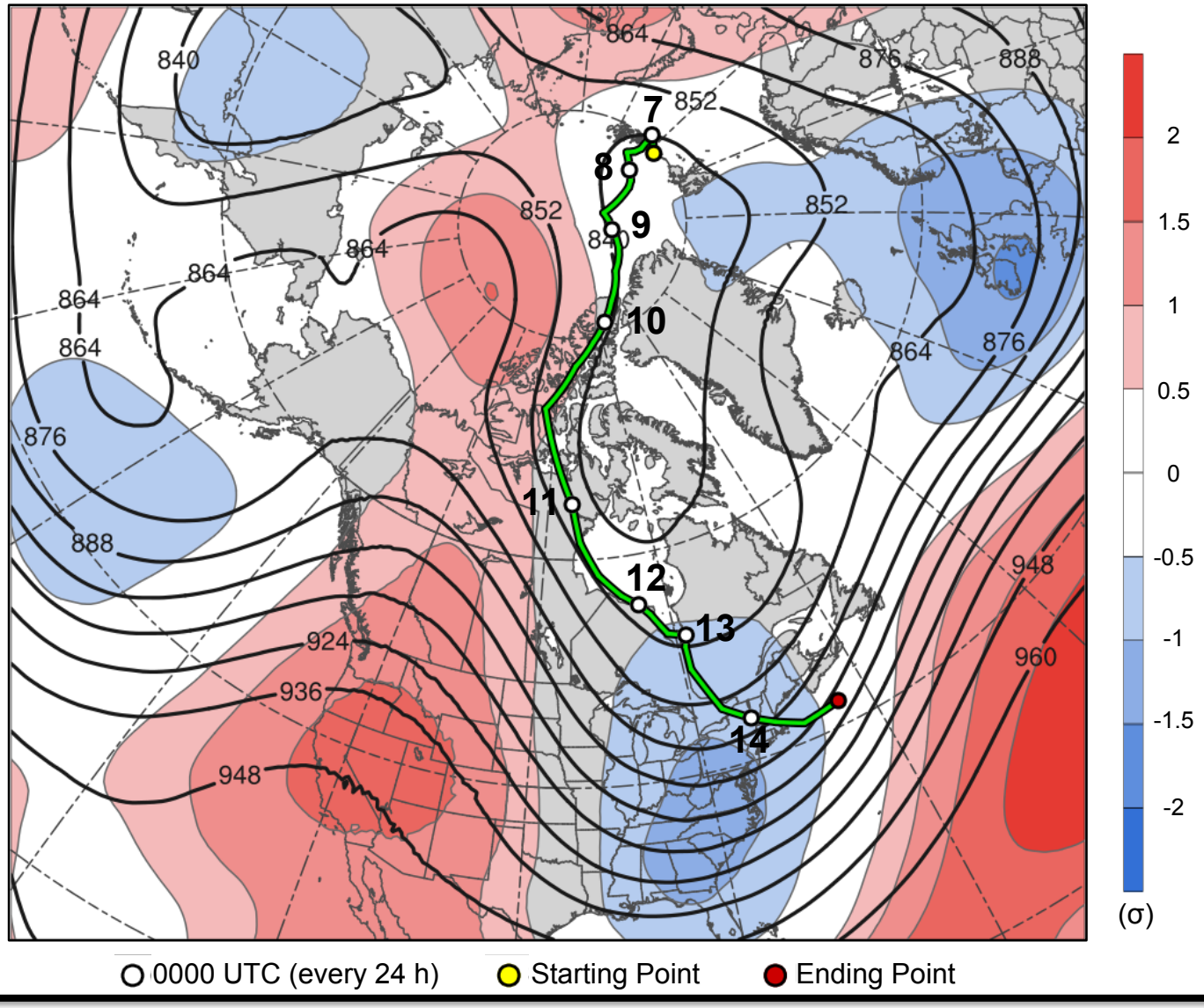

6–14 February 2016 time-mean 300-hPa geopotential height (dam, black) and standardized anomaly of geopotential height (σ, shaded)

Case 2: Upstream Ridge Evolution

0000 UTC 7 Feb 2016

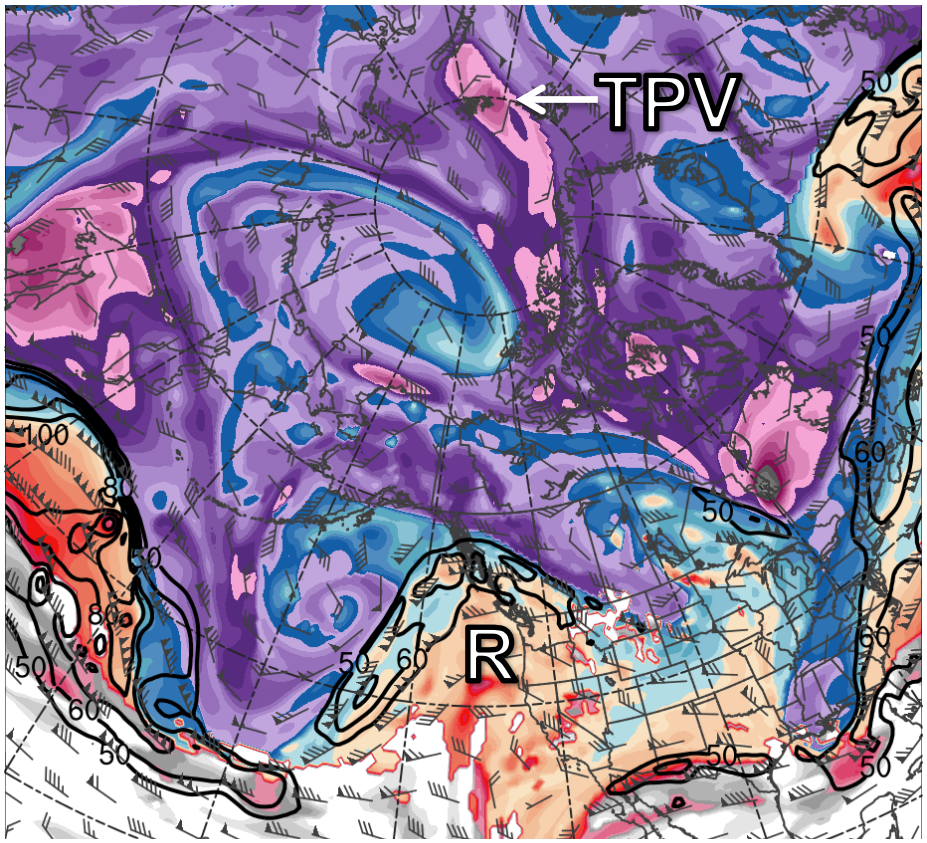

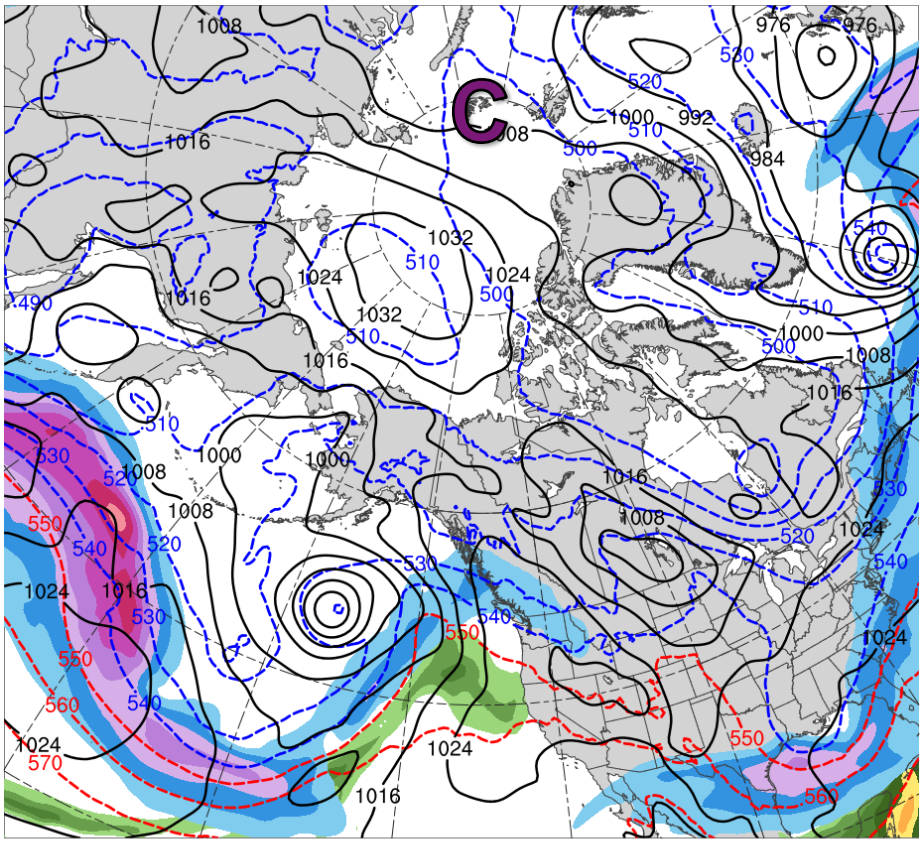

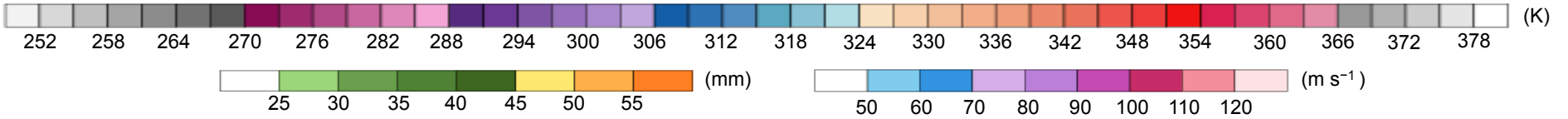

Potential temperature (K, shaded), wind speed (black, every 10 m s^{-1} starting at 50 m s^{-1}), and wind (m s^{-1}, barbs) on 2-PVU surface

250-hPa wind speed (m s^{-1}, shaded), 1000–500-hPa thickness (every 10 dam, blue/red), MSLP (every 8 hPa, black), PW (mm, shaded)

Case 2: Upstream Ridge Evolution

0000 UTC 9 Feb 2016

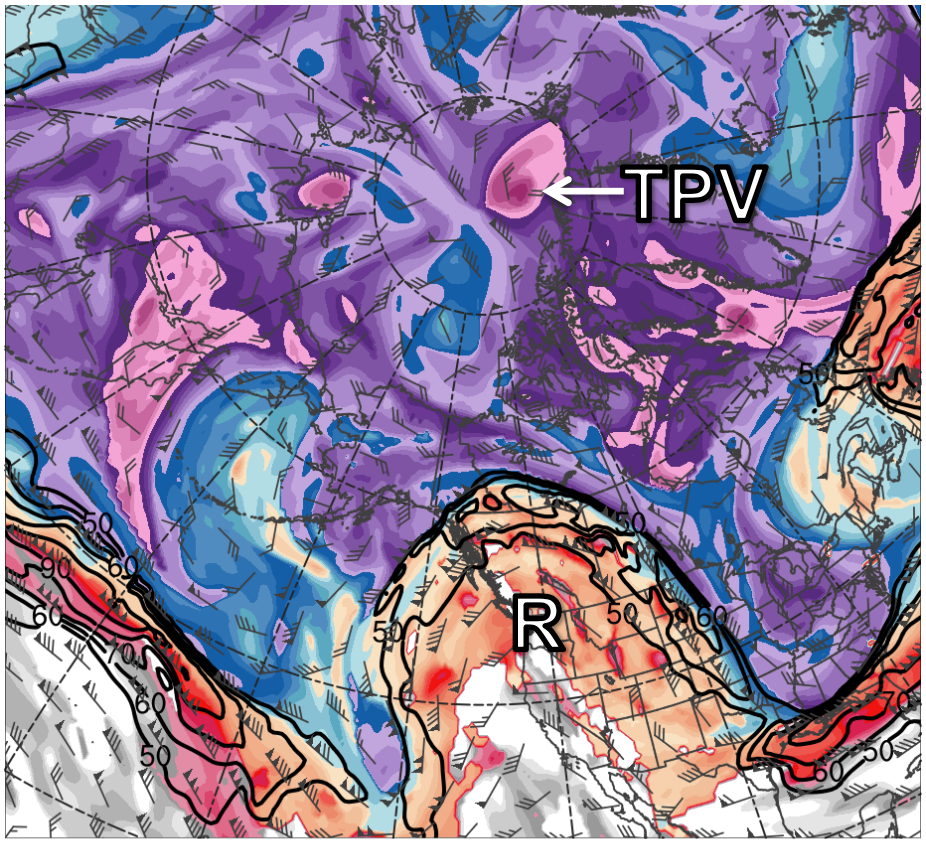

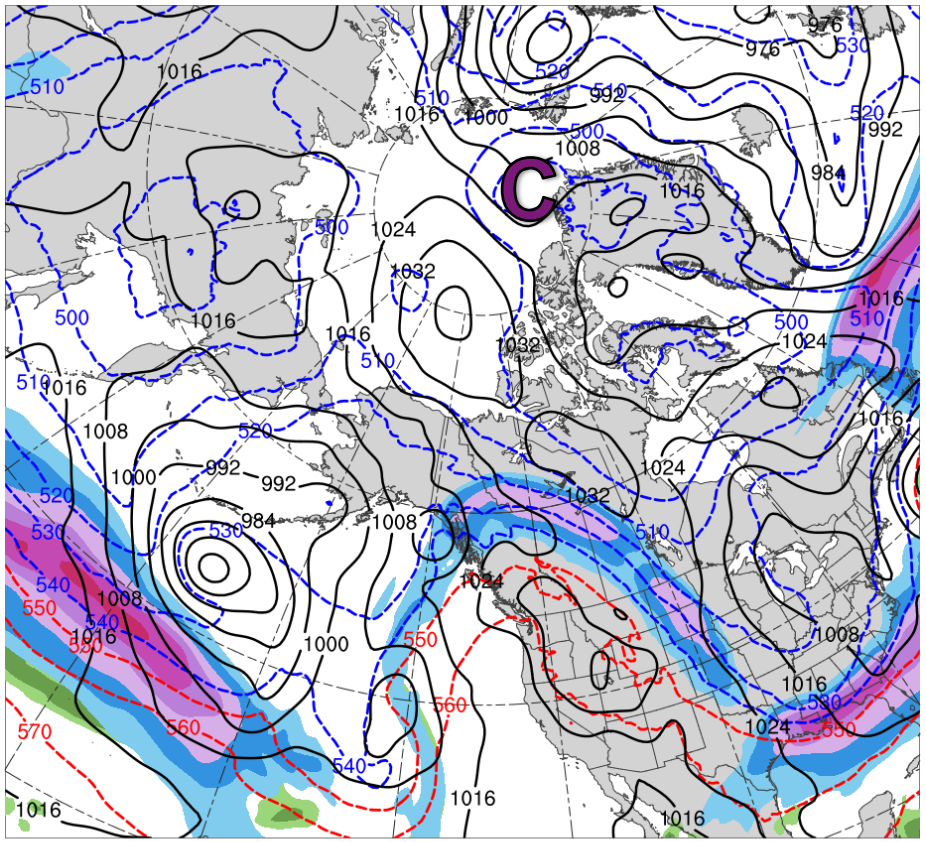

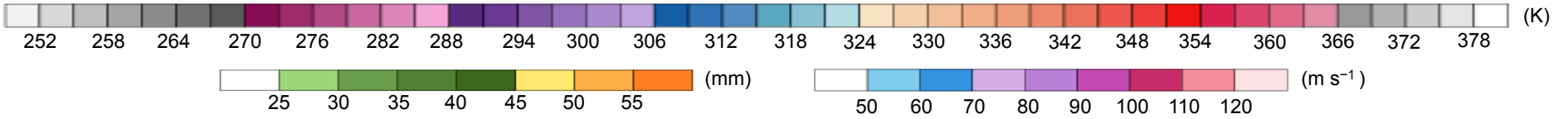

Potential temperature (K, shaded), wind speed (black, every 10 m s^{-1} starting at 50 m s^{-1}), and wind (m s^{-1}, barbs) on 2-PVU surface

250-hPa wind speed (m s^{-1}, shaded), 1000–500-hPa thickness (every 10 dam, blue/red), MSLP (every 8 hPa, black), PW (mm, shaded)

Case 2: Upstream Ridge Evolution

0000 UTC 11 Feb 2016

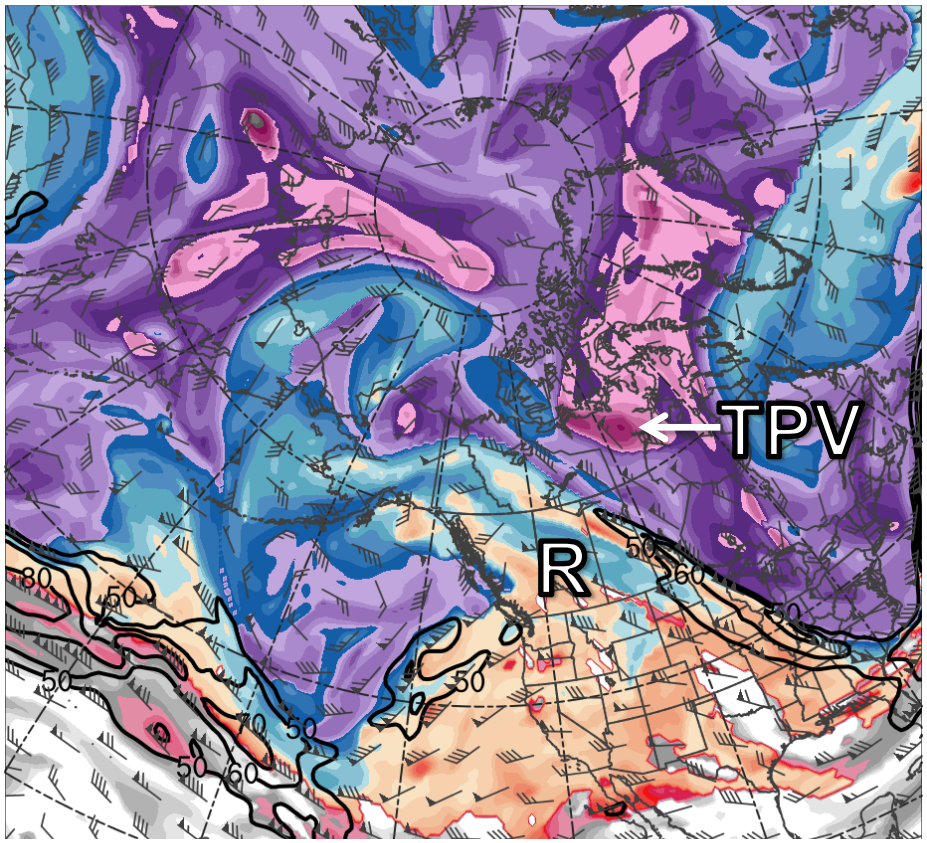

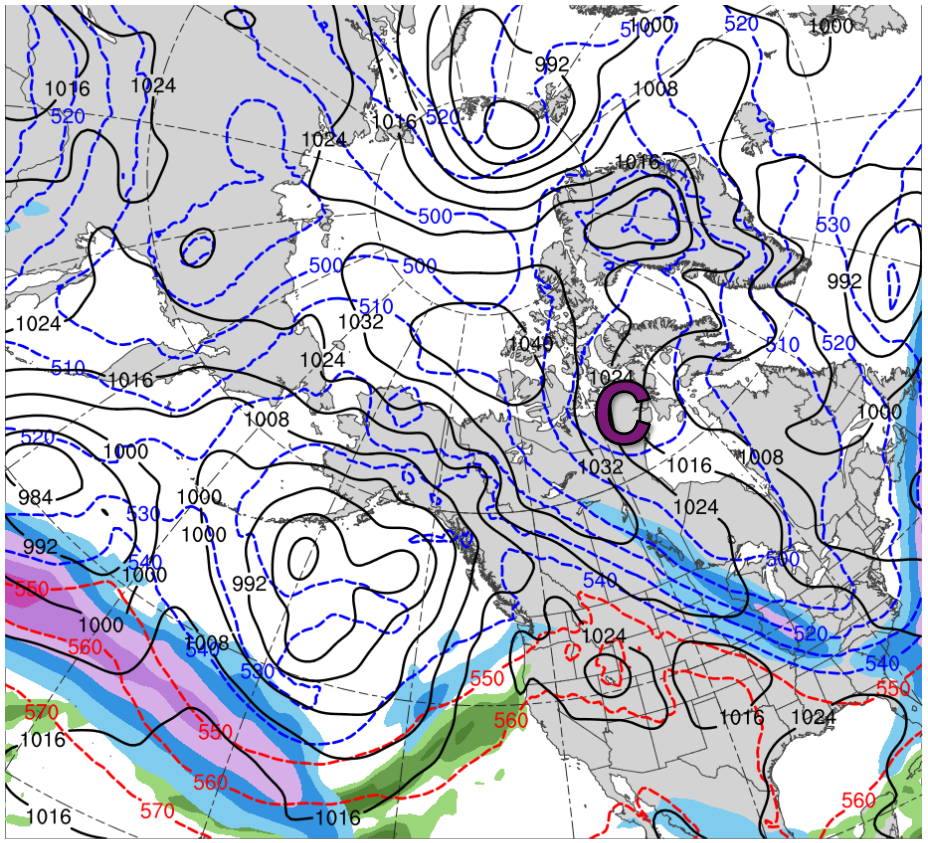

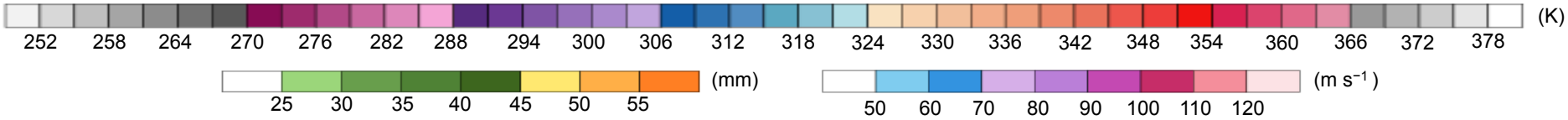

Potential temperature (K, shaded), wind speed (black, every 10 m s^{-1} starting at 50 m s^{-1}), and wind (m s^{-1}, barbs) on 2-PVU surface

250-hPa wind speed (m s^{-1}, shaded), 1000–500-hPa thickness (every 10 dam, blue/red), MSLP (every 8 hPa, black), PW (mm, shaded)

Case 2: TPV Transport and CAO

0000 UTC 12 Feb 2016

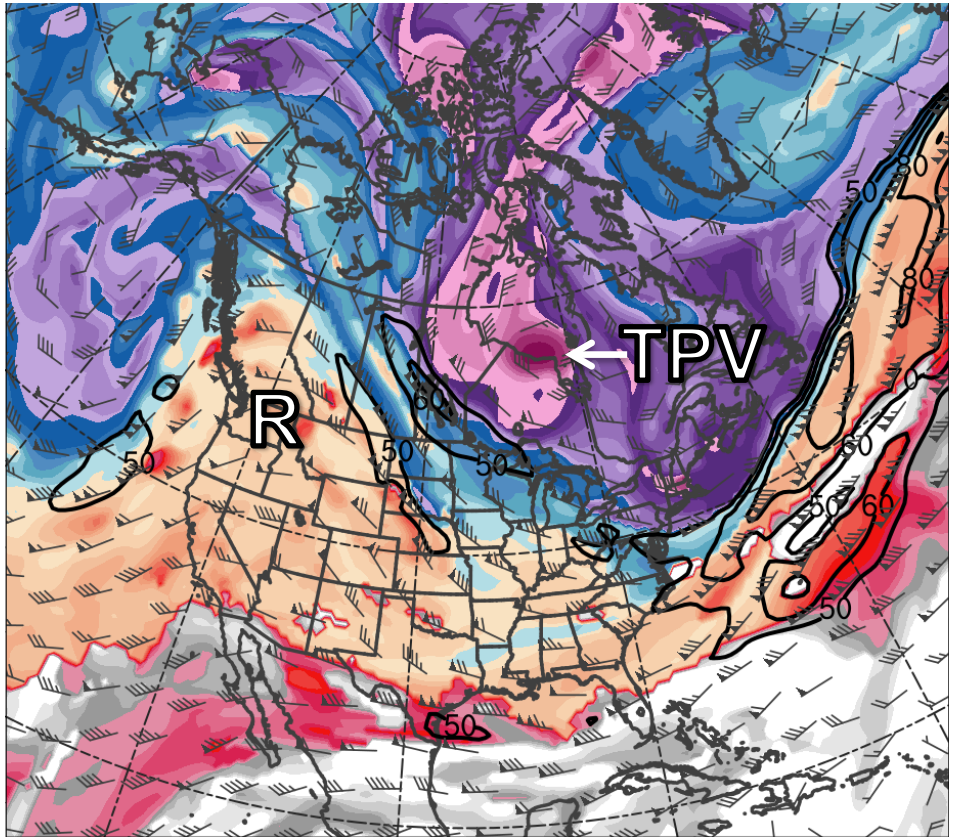

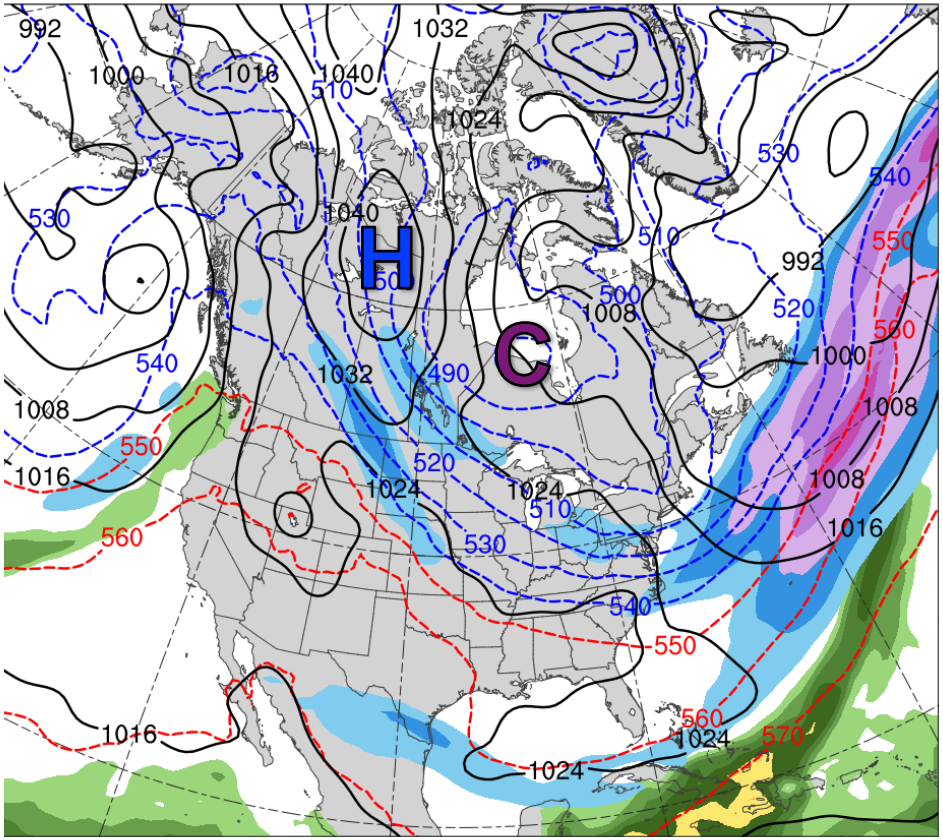

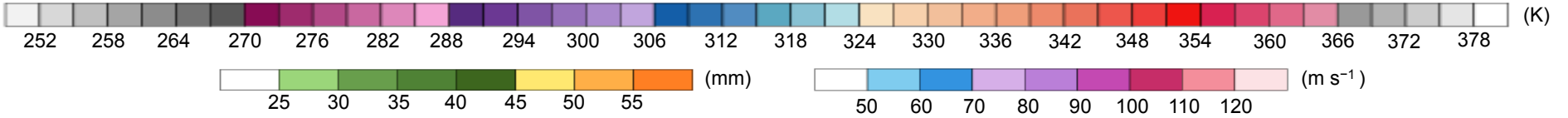

Potential temperature (K, shaded), wind speed (black, every 10 m s^{-1} starting at 50 m s^{-1}), and wind (m s^{-1}, barbs) on 2-PVU surface

250-hPa wind speed (m s^{-1}, shaded), 1000–500-hPa thickness (every 10 dam, blue/red), MSLP (every 8 hPa, black), PW (mm, shaded)

Case 2: TPV Transport and CAO

0000 UTC 13 Feb 2016

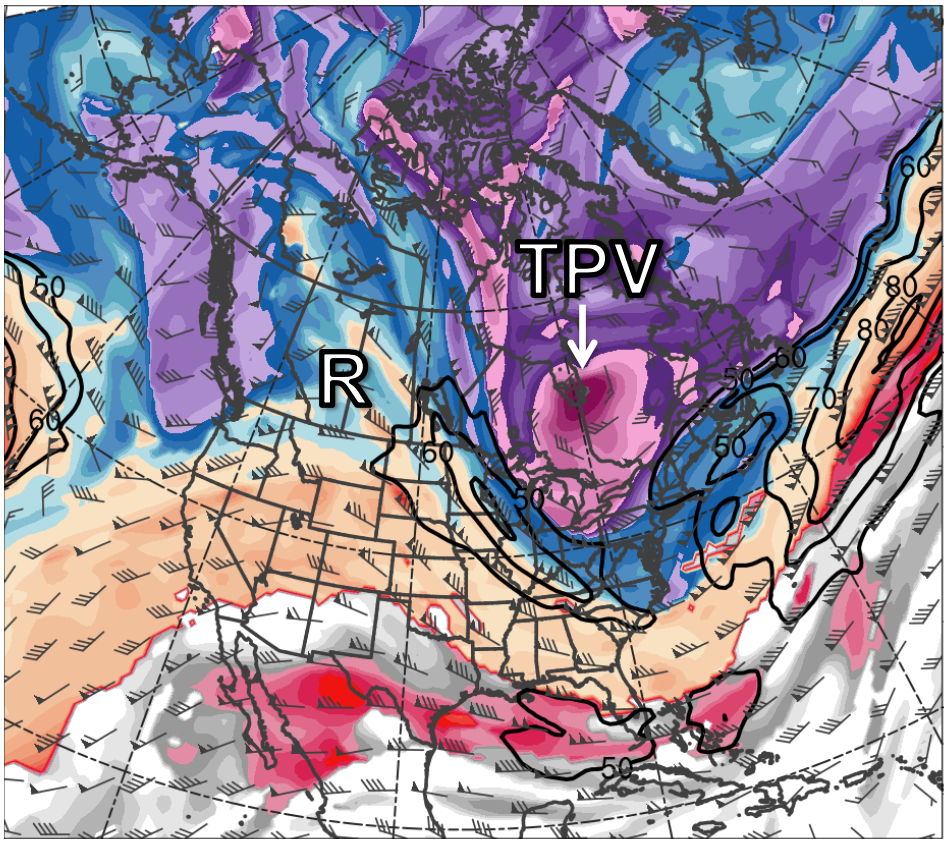

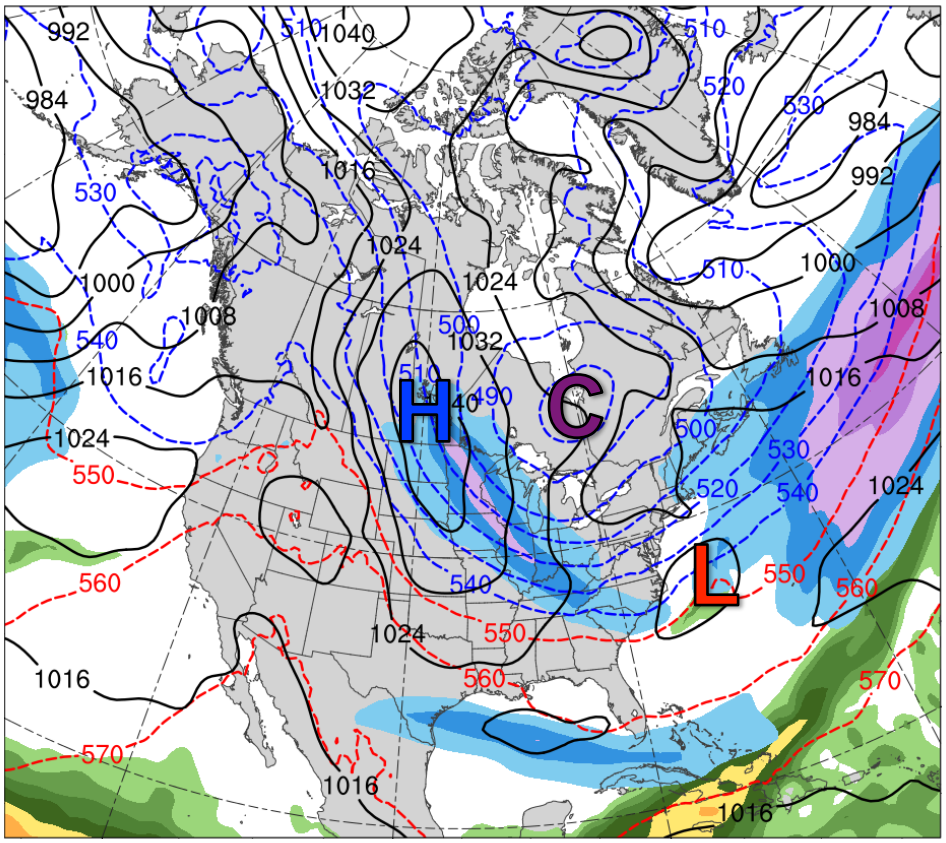

252 258 264 270 276 282 288 294 300 306 312 318 324 330 336 342 348 354 360 366 372 378 (K)

25 30 35 40 45 50 55 (mm)

50 60 70 80 90 100 110 120 (m s^{-1})

Potential temperature (K, shaded), wind speed (black, every 10 m s^{-1} starting at 50 m s^{-1}), and wind (m s^{-1}, barbs) on 2-PVU surface

250-hPa wind speed (m s^{-1}, shaded), 1000–500-hPa thickness (every 10 dam, blue/red), MSLP (every 8 hPa, black), PW (mm, shaded)

Case 2: TPV Transport and CAO

0000 UTC 14 Feb 2016

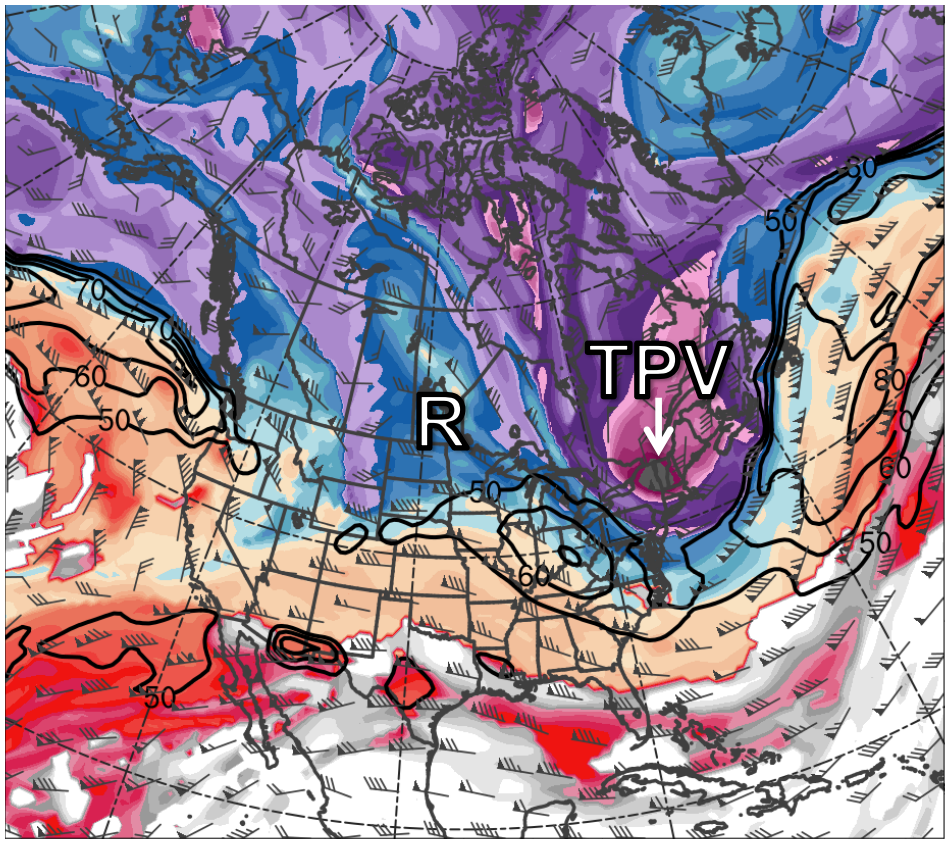

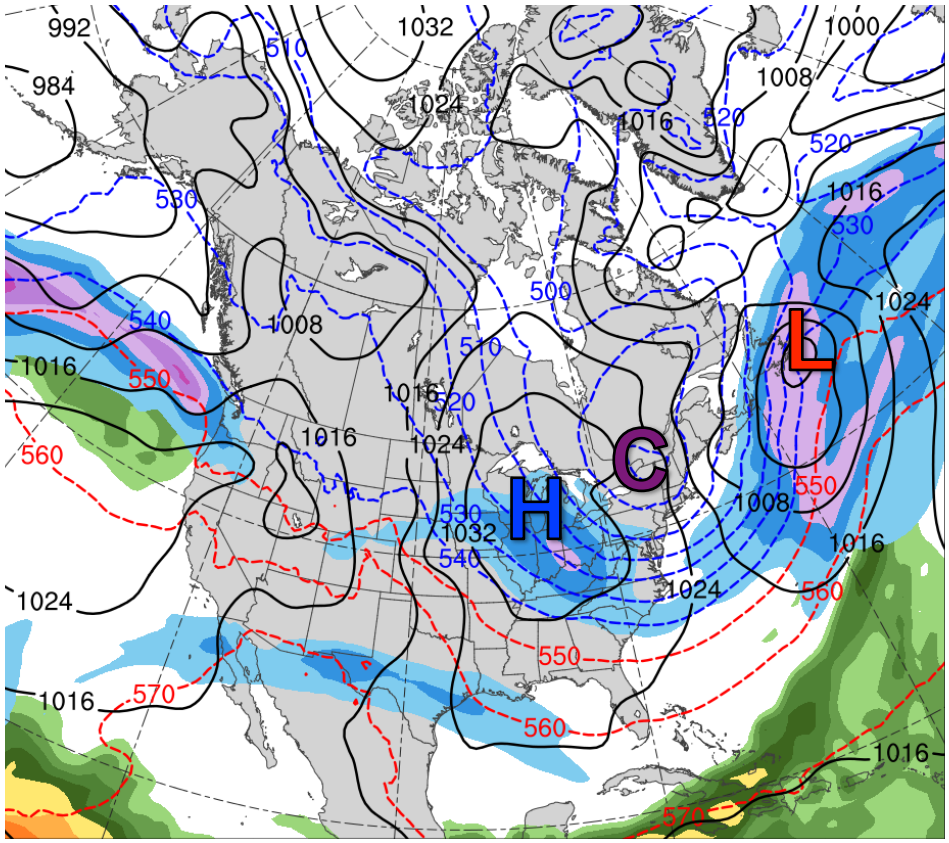

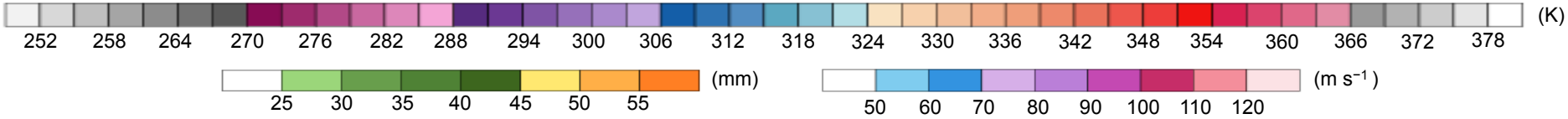

Potential temperature (K, shaded), wind speed (black, every 10 m s^{-1} starting at 50 m s^{-1}), and wind (m s^{-1}, barbs) on 2-PVU surface

250-hPa wind speed (m s^{-1}, shaded), 1000–500-hPa thickness (every 10 dam, blue/red), MSLP (every 8 hPa, black), PW (mm, shaded)

Case 2: Cross Section

0000 UTC 14 Feb 2016

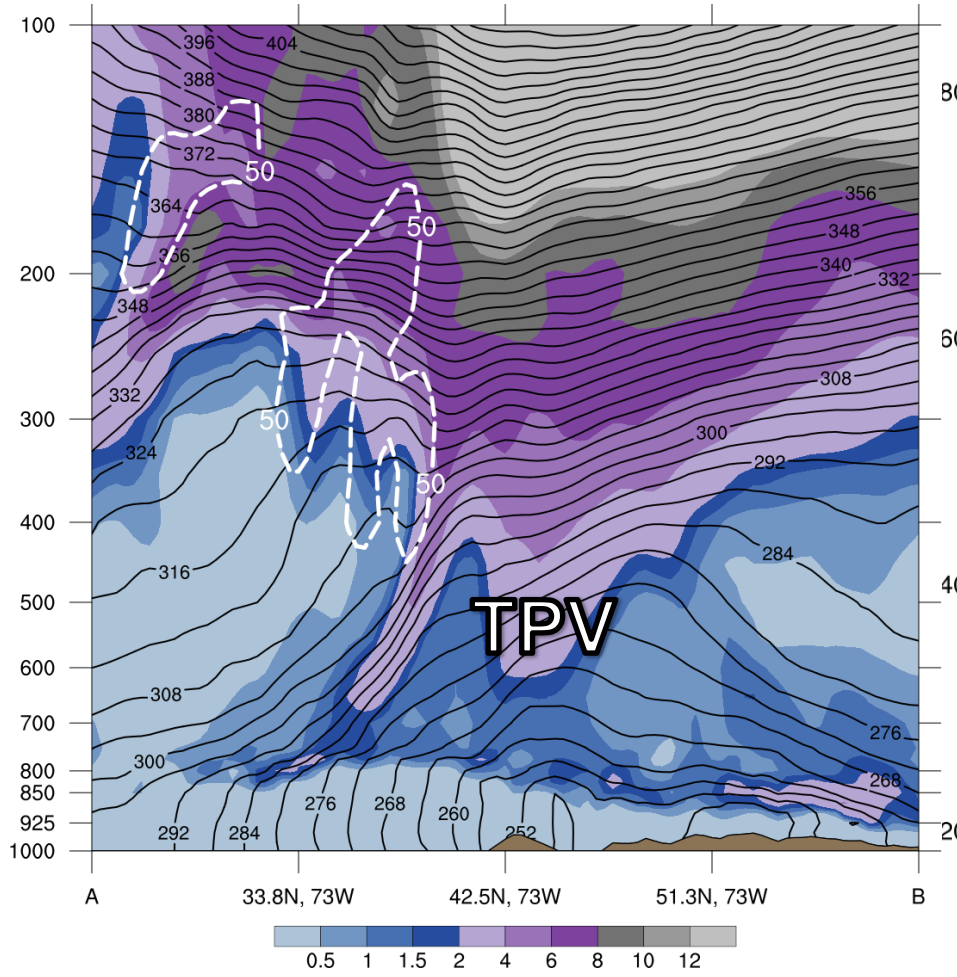

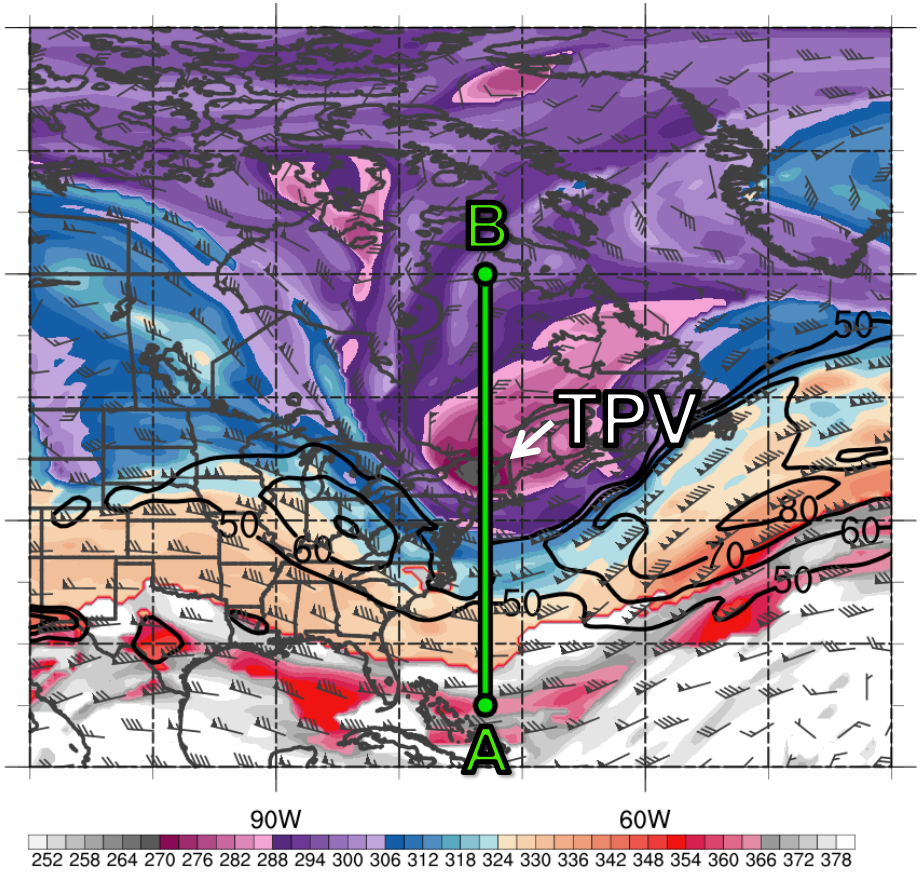

Potential vorticity (PVU, shaded), wind speed (white, every 10 m s^{-1} starting at 50 m s^{-1}), and potential temperature (K, black)

Potential temperature (K, shaded), wind speed (black, every 10 m s^{-1} starting at 50 m s^{-1}), and wind (m s^{-1}, barbs) on 2-PVU surface

Case 2: QG Diagnostics

1200 UTC 11 Feb 2016

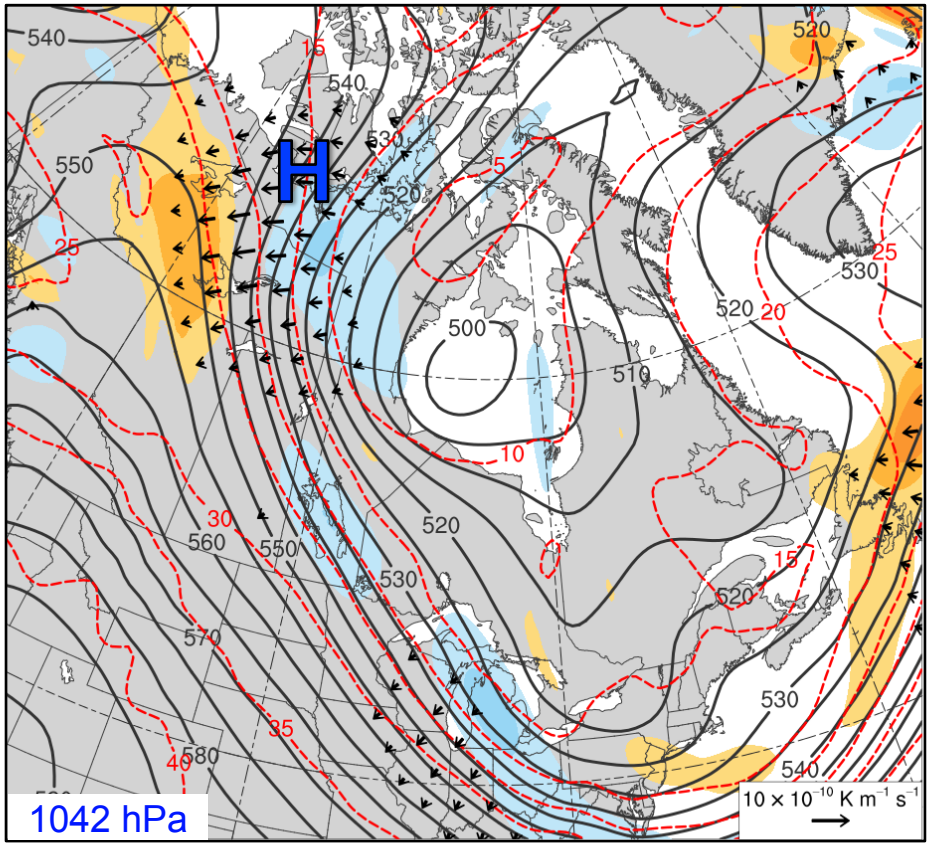

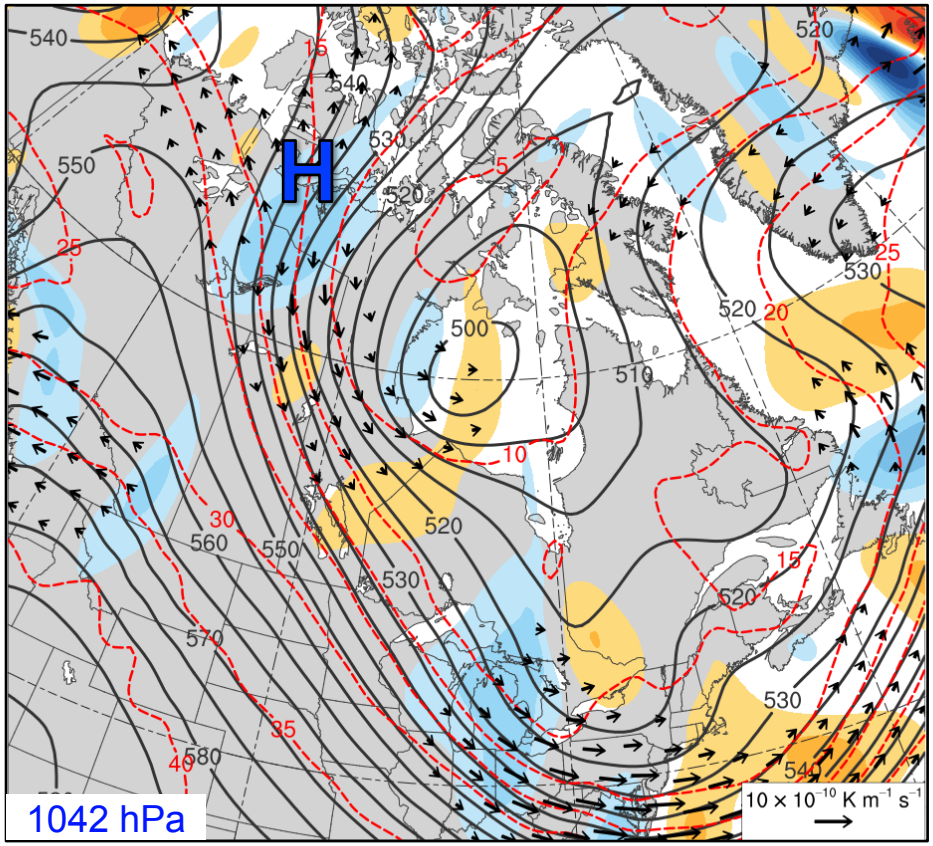

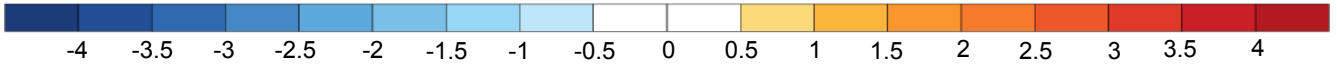

600–400-hPa layer averaged $\mathbf{Q}_n$ (K m^{-1} s^{-1}, vectors), $\mathbf{Q}_n$ forcing for vertical motion (×10^{-18} Pa^{-1} s^{-3}, shaded), geopotential height (dam, gray), and potential temperature (K, red)

600–400-hPa layer averaged $\mathbf{Q}_s$ (K m^{-1} s^{-1}, vectors), $\mathbf{Q}_s$ forcing for vertical motion (×10^{-18} Pa^{-1} s^{-3}, shaded), geopotential height (dam, gray), and potential temperature (K, red)

Case 2: QG Diagnostics

0000 UTC 12 Feb 2016

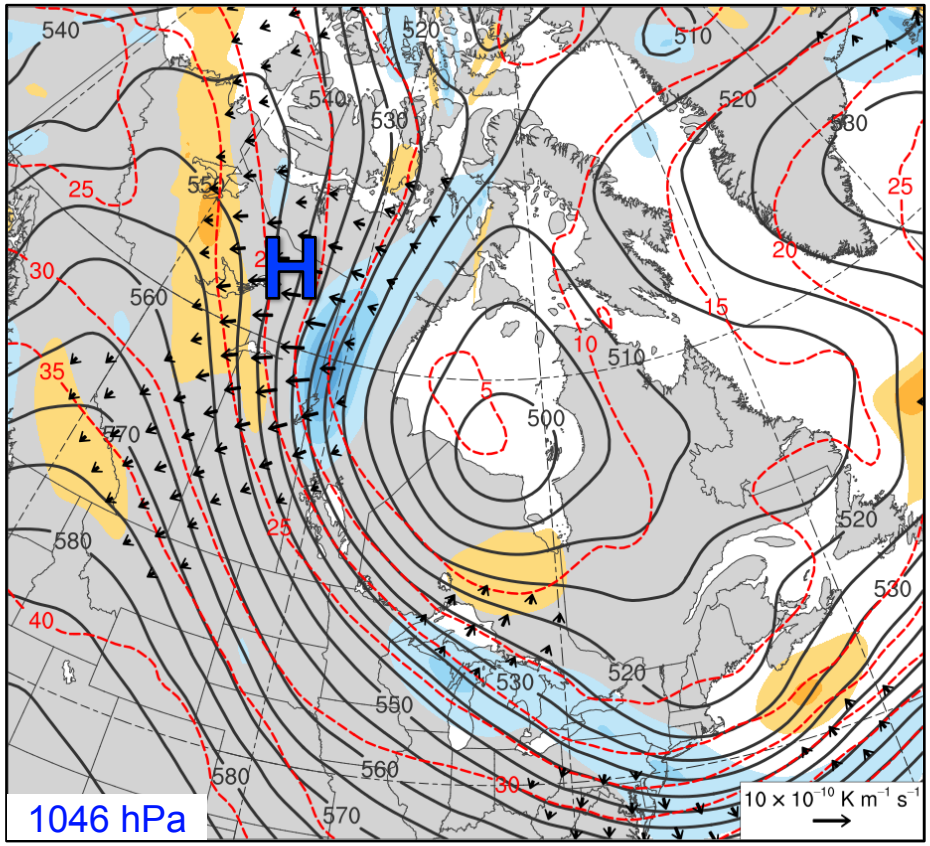

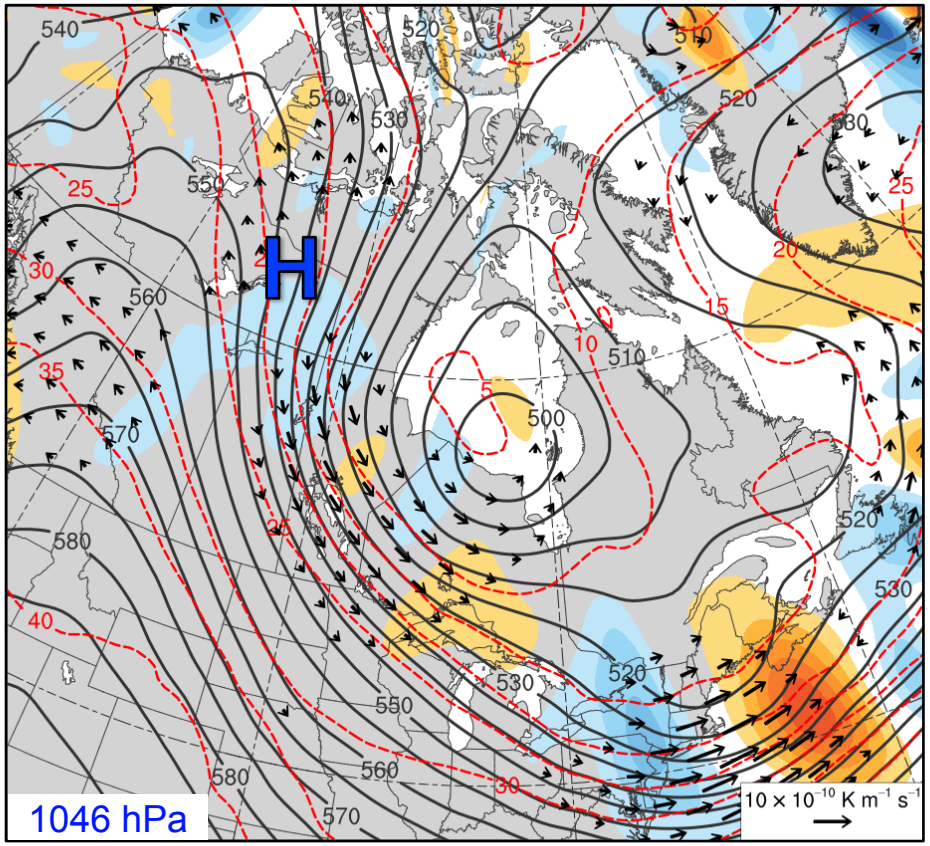

-4 -3.5 -3 -2.5 -2 -1.5 -1 -0.5 0 0.5 1 1.5 2 2.5 3 3.5 4

600–400-hPa layer averaged $\mathbf{Q}_n$ (K m^{-1} s^{-1}, vectors), $\mathbf{Q}_n$ forcing for vertical motion (×10^{-18} Pa^{-1} s^{-3}, shaded), geopotential height (dam, gray), and potential temperature (K, red)

600–400-hPa layer averaged $\mathbf{Q}_s$ (K m^{-1} s^{-1}, vectors), $\mathbf{Q}_s$ forcing for vertical motion (×10^{-18} Pa^{-1} s^{-3}, shaded), geopotential height (dam, gray), and potential temperature (K, red)

Case 2: QG Diagnostics

0000 UTC 12 Feb 2016

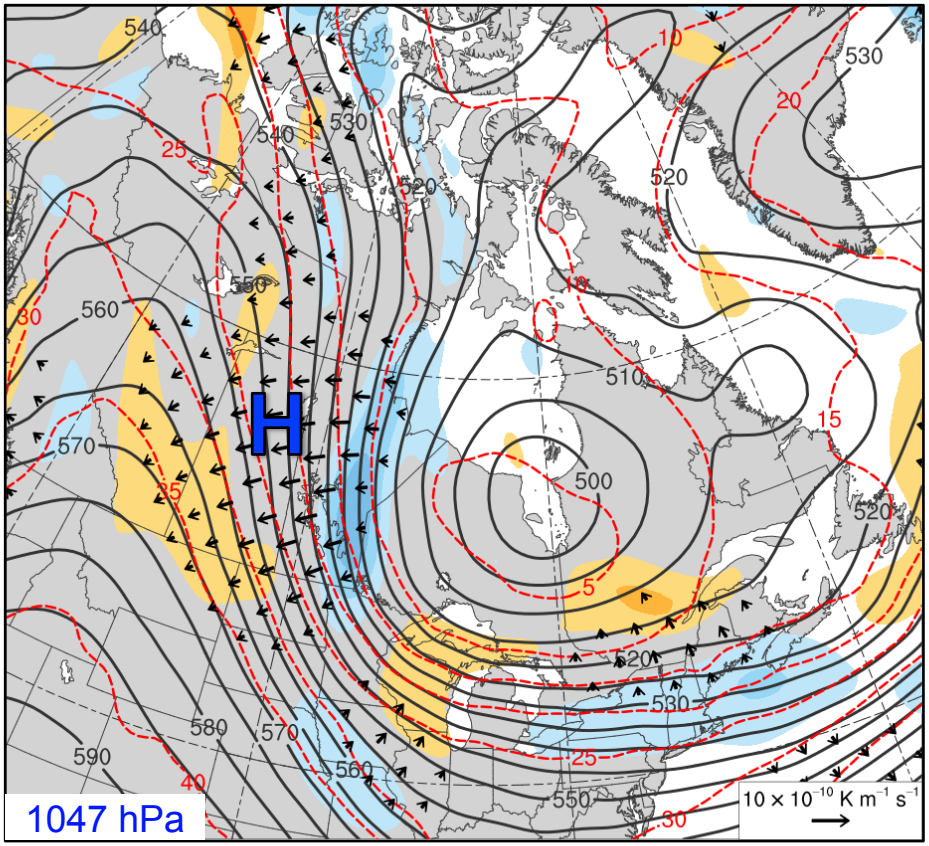

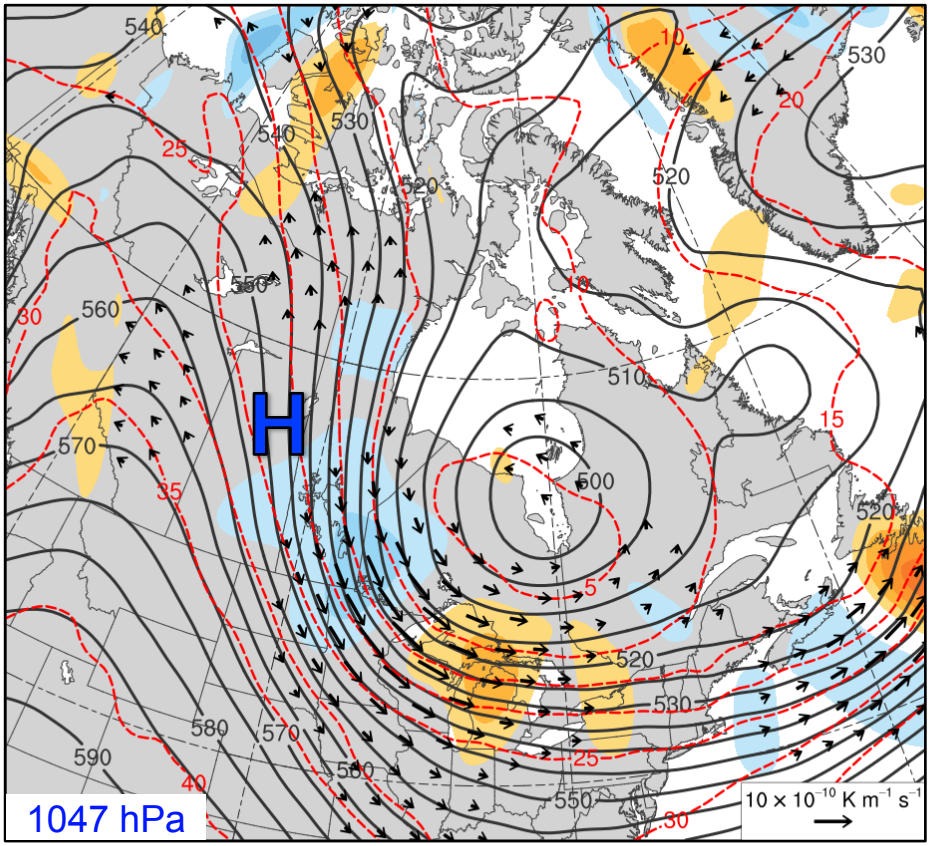

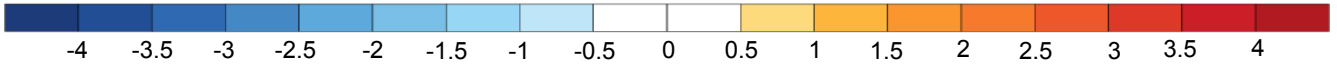

600–400-hPa layer averaged $\mathbf{Q}_n$ (K m^{-1} s^{-1}, vectors), $\mathbf{Q}_n$ forcing for vertical motion (×10^{-18} Pa^{-1} s^{-3}, shaded), geopotential height (dam, gray), and potential temperature (K, red)

600–400-hPa layer averaged $\mathbf{Q}_s$ (K m^{-1} s^{-1}, vectors), $\mathbf{Q}_s$ forcing for vertical motion (×10^{-18} Pa^{-1} s^{-3}, shaded), geopotential height (dam, gray), and potential temperature (K, red)

Conclusions

- Extratropical cyclones in exit region of North Pacific jet play important role in downstream development and amplification or ridges responsible for equatorward TPV transport in both cases

- Both TPVs collocated with surface-based pool of arctic air, with an arctic frontal feature extending downward and equatorward from TPVs

- January 1982 case, in particular, indicates that TPV–jet interactions may enhance QG forcing for descent in jet entrance region, supporting intensification of surface anticyclone in this region

- February 2016 TPV interacts less with upstream jet, and overall QG forcing for descent is weaker near surface anticyclone in this case compared to January 1982 case

Conclusions

- Stronger surface anticyclones may be associated with stronger downstream MSLP gradient
- Equatorward transport of surface-based pools of arctic air associated with TPVs may lead to enhanced thermal gradients over middle latitudes
- Stronger MSLP and thermal gradients may lead to stronger cold air advection
- Regardless, as surface-based pools of arctic air beneath and behind TPVs moves equatorward along with TPVs into middle latitudes, CAOs may result